

# KP solitons, higher Bruhat and Tamari orders

ARISTOPHANES DIMAKIS

Department of Financial and Management Engineering,  
University of the Aegean, 41, Kountourioti Str., GR-82100 Chios, Greece  
E-mail: *dimakis@aegean.gr*

FOLKERT MÜLLER-HOISSEN

Max-Planck-Institute for Dynamics and Self-Organization  
Bunsenstrasse 10, D-37073 Göttingen, Germany  
E-mail: *folkert.mueller-hoissen@ds.mpg.de*

## Abstract

In a tropical approximation, any tree-shaped line soliton solution, a member of the simplest class of soliton solutions of the Kadomtsev-Petviashvili (KP-II) equation, determines a chain of planar rooted binary trees, connected by right rotation. More precisely, it determines a maximal chain of a Tamari lattice. We show that an analysis of these solutions naturally involves higher Bruhat and higher Tamari orders.

## 1 Introduction

Waves on a fluid surface show a very complex behavior in general. Only under special circumstances can we expect to observe a more regular pattern. For shallow water waves, the Kadomtsev-Petviashvili (KP) equation

$$(-4u_t + u_{xxx} + 6uu_x)_x + 3u_{yy} = 0$$

(where e.g.  $u_t = \partial u / \partial t$ ) provides an approximation under the conditions that the wave dominantly travels in the  $x$ -direction, the wave length is long as compared with the water depth, and the effect of the nonlinearity is about the same order as that of dispersion.<sup>1</sup> More precisely, this is the KP-II equation, but we will write KP, for short. It generalizes the famous Korteweg-deVries (KdV) equation, which describes waves moving in only one spatial dimension. Although the KdV equation is much better established as an approximation of the more general water wave equations, recent studies also confirm the physical relevance of KP [9].

In [2] we studied the soliton solutions of the KP equation in a *tropical* approximation, which reduces them to networks formed by line segments in the  $xy$ -plane, evolving in time  $t$ . A subclass corresponds to evolutions (in time  $t$ ) in the set of (planar) rooted binary trees. At transition events, the binary tree type changes (through a tree that is not binary). It turned out that the time evolution is simply given by right rotation in a tree, and the solution evolves according to a maximal chain of a *Tamari lattice* [24, 25], see Figure 1.

<sup>1</sup>The physical form of this equation is obtained by suitable rescalings of  $x, y, t$  and  $u$ , involving physical parameters.

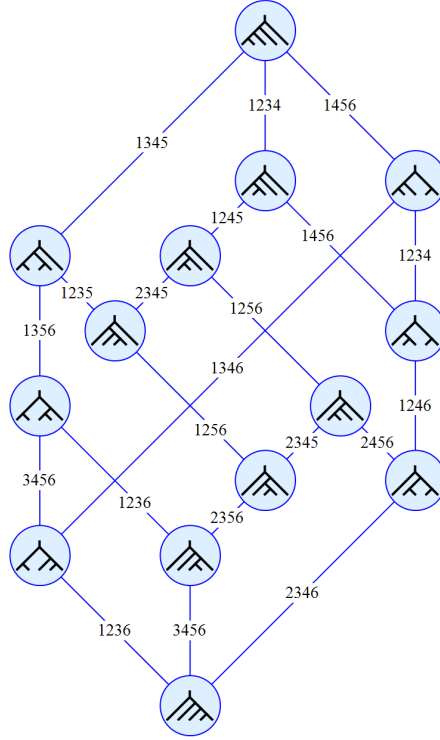


Figure 1: The Tamari lattice  $\mathbb{T}_4$  in terms of rooted binary trees. The top node shows a left comb tree that represents the structure of a certain KP line soliton family (with six asymptotic branches in the  $xy$ -plane) as  $t \rightarrow -\infty$ . A label  $ijkl$  assigned to an edge indicates the transition time  $t_{ijkl}$  at which the soliton graph changes its tree type via a ‘rotation’ (see Section 3). The values of the parameters, on which the solutions depend, determine the linear order of the ‘critical times’  $t_{ijkl}$ , and thus decide which chain is realized. The bottom node shows a right comb tree, which represents the tree type of the soliton as  $t \rightarrow \infty$ . The special family of solutions thus splits into classes corresponding to the maximal chains of  $\mathbb{T}_4$ . For each Tamari lattice, there is a family of KP line solitons that realizes its maximal chains in this way.

In this realization of Tamari lattices, the underlying set consists of states of a physical system, here the tree-types of a soliton configuration in the  $xy$ -plane. The Tamari poset (partially ordered set) structure describes the possible ways in which these states are allowed to evolve in time, starting from an initial state (the top node) and ending in a final state (the bottom node).

Figure 2 displays a solution evolving via a tree rotation, and further provides an idea how this can be understood in terms of an arrangement of planes in three-dimensional space-time (after idealizing line soliton branches to lines in the  $xy$ -plane, see Section 3).

In this work we show that the classification of possible evolutions of tree-shaped KP line solitons involves *higher Bruhat orders* [17–19, 30]. Moreover, we are led to associate with each higher Bruhat order a *higher Tamari order* via a surjection, in a way different from what has been considered previously. There is some evidence that our higher Tamari orders coincide with ‘higher Stasheff-Tamari posets’ introduced by Kapranov and Voevodsky [8] (also see [3]), but a closer comparison will not be undertaken in this work.

In Section 2, we briefly describe the general class of KP soliton solutions. In Section 3, we concentrate on the abovementioned subclass of tree-shaped solutions, in the tropical approximation, and somewhat improve results in [2]. Section 4 recalls results about higher Bruhat orders and extracts from the analysis of tree-shaped KP line solitons a reduction to higher Tamari orders. Section 7 proposes a hierarchy of monoids

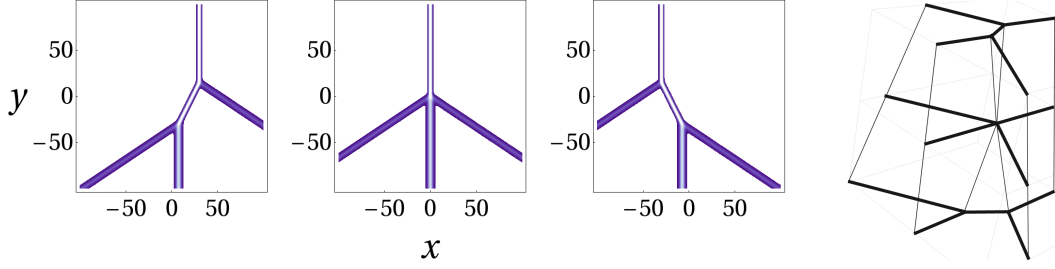


Figure 2: Density plots of a line soliton solution at three successive times, exhibiting a tree rotation. To the right is a corresponding space-time view in terms of intersecting planes (here time flows upward).

that expresses the hierarchical structure present in the KP soliton problem. This makes contact with *simplex equations* [1, 6, 13, 29] and provides us with an algebraic method to construct higher Bruhat and higher Tamari orders. Section 8 contains some additional remarks. Throughout this work, Hasse diagrams of posets will be displayed upside down (i.e. with the lowest element(s) at the top).

## 2 KP solitons

The line soliton solutions of the KP-II equation are parametrized by the totally non-negative Grassmannians  $\text{Gr}_{n, M+1}^{\geq}$  [9], which is easily recognized in the Wronskian form of the solutions. Translating the KP equation via

$$u = 2 \log(\tau)_{xx},$$

into a bilinear equation in the variable  $\tau$ , these solutions are given by

$$\tau = f_1 \wedge f_2 \wedge \cdots \wedge f_n,$$

where

$$f_i = \sum_{j=1}^{M+1} a_{ij} e_j, \quad e_j = e^{\theta_j}, \quad \theta_j = \sum_{r=1}^M p_j^r t^{(r)} + c_j.$$

Here  $t^{(r)}$ ,  $r = 1, \dots, M$ , are independent real variables that may be regarded as coordinates on  $\mathbb{R}^M$ , and we set  $t^{(1)} = x$ ,  $t^{(2)} = y$ ,  $t^{(3)} = t$ . The variables  $t^{(r)}$ ,  $r > 3$ , are the additional evolution variables that appear in the *KP hierarchy*, which extends the KP equation to an infinite set of compatible PDEs. Furthermore,  $p_j, c_j, a_{ij}$  are real constants, and without restriction of generality we can and will assume that

$$p_1 < p_2 < \cdots < p_{M+1}.$$

The exterior product on the space of functions generated by the exponential functions  $e_j$ ,  $j = 1, \dots, M+1$ , is defined by

$$e_{i_1} \wedge \cdots \wedge e_{i_m} = \Delta(p_{i_1}, \dots, p_{i_m}) e_{i_1} \cdots e_{i_m},$$

with the Vandermonde determinant

$$\Delta(p_{i_1}, \dots, p_{i_m}) = \begin{vmatrix} 1 & p_{i_1} & \cdots & p_{i_1}^{m-1} \\ 1 & p_{i_2} & \cdots & p_{i_2}^{m-1} \\ \vdots & \vdots & \cdots & \vdots \\ 1 & p_{i_m} & \cdots & p_{i_m}^{m-1} \end{vmatrix} = \prod_{1 \leq r < s \leq m} (p_{i_s} - p_{i_r}).$$

Now we can express  $\tau$  as

$$\tau = \sum_{I \in \binom{[M+1]}{n}} A_I \Delta(p_I) e_I,$$

where  $[m] = \{1, 2, \dots, m\}$ , and  $\binom{[m]}{n}$  denotes the set of  $n$ -element subsets of  $[m]$ . Numbering the elements of a subset  $I = \{i_1, \dots, i_n\}$  such that  $i_1 < \dots < i_n$ , we set  $\Delta(p_I) = \Delta(p_{i_1}, \dots, p_{i_n})$ . Finally,  $A_I$  denotes the maximal minor with columns  $i_1, \dots, i_n$  of the matrix

$$A = \begin{pmatrix} a_{1,1} & \cdots & a_{1,M+1} \\ \vdots & \ddots & \vdots \\ a_{n,1} & \cdots & a_{n,M+1} \end{pmatrix}.$$

For regular (soliton) solutions, the Plücker coordinates  $A_I$  have to be *non-negative* real numbers (and at least one has to be different from zero). In the following we concentrate on the subclass of solutions parametrized by  $\text{Gr}_{1,M+1}^{\geq}$ , i.e.

$$\tau = e_1 + \cdots + e_{M+1}, \quad (1)$$

where we absorbed the positive constants  $a_{1,j}$  into the constants  $c_j$ . To good approximation, a *general* line soliton solution can be understood as a *superimposition* of solutions from the subclass (see [2]).

### 3 Tropical approximation of a subclass of KP line solitons

Let us fix  $M \in \mathbb{N}$ , constants  $p_1 < p_2 < \cdots < p_{M+1}$  and  $c_i, i = 1, \dots, M+1$ . The behavior of  $\tau : \mathbb{R}^M \rightarrow \mathbb{R}$ , given by (1), is best understood in a tropical approximation of  $\log(\tau)$ . In a region where some phase, say  $\theta_i$ , *dominates* all others, i.e.  $\theta_i > \theta_j$  for all  $j \neq i$ , we have

$$\log(\tau) = \theta_i + \log \left( 1 + \sum_{\substack{j=1 \\ j \neq i}}^{M+1} e^{-(\theta_i - \theta_j)} \right) \simeq \theta_i.$$

As a consequence,

$$\log(\tau) \simeq \max\{\theta_1, \dots, \theta_{M+1}\},$$

where the right hand side can be regarded as a *tropical* version of  $\log(\tau)$ . Sufficiently away from the boundary of a dominating-phase region,  $\log(\tau)$  is linear in  $x$ , so that  $u$  vanishes. A crucial observation is that a line soliton branch in the  $xy$ -plane, for fixed  $t^{(r)}$ ,  $r > 2$ , corresponds to a boundary line between two dominating-phase regions. Viewing it in space-time, by regarding  $t$  as a coordinate of an additional dimension, or more generally in the extended space  $\mathbb{R}^M$  by adding dimensions corresponding to the evolution variables  $t^{(r)}$ ,  $r = 3, \dots, M$ , the boundary consists piecewise of affine hyperplanes. Let  $\mathcal{U}_i$  denote the region where  $\theta_i$  is not dominated by any other phase, i.e.

$$\mathcal{U}_i = \{\mathbf{t} \in \mathbb{R}^M \mid \max\{\theta_1, \dots, \theta_{M+1}\} = \theta_i\} = \bigcap_{k \neq i} \{\mathbf{t} \in \mathbb{R}^M \mid \theta_k \leq \theta_i\}. \quad (2)$$

In the tropical approximation, a description of KP line solitons amounts to an analysis of intersections of such regions, i.e.

$$\mathcal{U}_I = \mathcal{U}_{i_1} \cap \cdots \cap \mathcal{U}_{i_n}, \quad I = \{i_1, \dots, i_n\} \in \binom{[M+1]}{n}, \quad \Omega := [M+1] = \{1, \dots, M+1\}.$$

This is a subset of the affine space

$$\mathcal{P}_I = \{\mathbf{t} \in \mathbb{R}^M \mid \theta_{i_1} = \dots = \theta_{i_n}\} \quad n > 1,$$

which is easy to deal with (see below). It is more difficult to determine which parts of  $\mathcal{P}_I$  are *visible*, i.e. belong to  $\mathcal{U}_I$ . Fixing the values of  $t^{(r)}$ ,  $r > 2$ , determines a line soliton segment in the  $xy$ -plane if  $n = 2$ , and a meeting point of  $n$  such segments if  $n > 2$ .<sup>2</sup> In order to decide about visibility, i.e. whether a point of  $\mathcal{P}_I$  lies in  $\mathcal{U}_I$ , a formula is needed to compare the values of all phases at this point, see (6) below.

Let us first look at  $\mathcal{P}_I$  in more detail. Introducing a real *auxiliary variable*  $t^{(0)}$ , the equation  $\theta_{i_1} = \dots = \theta_{i_n} = -t^{(0)}$  results in the linear system<sup>3</sup>

$$t^{(0)} + p_{i_j} t^{(1)} + p_{i_j}^2 t^{(2)} + \dots + p_{i_j}^{n-1} t^{(n-1)} = -\tilde{c}_{i_j}, \quad j = 1, \dots, n,$$

where

$$\tilde{c}_{i_j} = c_{i_j} + p_{i_j}^n t^{(n)} + \dots + p_{i_j}^M t^{(M)}.$$

This fixes the first  $n-1$  coordinates as linear functions of the remaining coordinates,  $t_I^{(k)} = t_I^{(k)}(t^{(n)}, \dots, t^{(M)})$ ,  $k = 1, \dots, n-1$ . In particular, we obtain (also see [2], Appendix A)

$$\begin{aligned} t_I^{(n-1)} &= - \sum_{r=1}^{M+1-n} h_r(p_I) t^{(n+r-1)} - c_I \\ &= -(p_{i_1} + \dots + p_{i_n}) t^{(n)} - \tilde{c}_I, \end{aligned} \quad (3)$$

where  $h_r(p_I) = h_r(p_{i_1}, \dots, p_{i_n})$  is the  $r$ -th *complete symmetric polynomial* [15] in the variables  $p_{i_1}, \dots, p_{i_n}$ , and

$$c_I = \frac{1}{\Delta(p_I)} \sum_{s=1}^n (-1)^{n-s} c_{i_s} \Delta(p_{I \setminus \{i_s\}}), \quad \tilde{c}_I = \sum_{r=2}^{M+1-n} h_r(p_I) t^{(n+r-1)} + c_I.$$

We note that  $\tilde{c}_I$  depends on  $t^{(n+1)}, \dots, t^{(M)}$ . Here are some immediate consequences:

- Since obviously  $\mathcal{P}_I \subset \mathcal{P}_J$  for  $J \subset I$ , on  $\mathcal{P}_I$  we have

$$t_I^{(n-2)} = t_{I \setminus \{i_n\}}^{(n-2)}(t_I^{(n-1)}, t^{(n)}, \dots, t^{(M)}),$$

and corresponding expressions for  $t_I^{(r)}$ ,  $r = 1, \dots, n-3$ .

- $\mathcal{P}_\Omega$  is a common point of all  $\mathcal{P}_I$ ,  $I \subset \Omega$ . According to (3), on  $\mathcal{P}_\Omega$  we have

$$t_\Omega^{(M)} = -c_\Omega.$$

Clearly,  $\mathcal{P}_\Omega = \mathcal{U}_\Omega$ , and is thus visible.

<sup>2</sup>For generic values of  $t^{(r)}$ ,  $r > 2$ , we see line soliton segments and meeting points of *three* segments in the  $xy$ -plane. Meeting points of more than three segments only occur for special values.

<sup>3</sup>We note that the full set of equations  $t^{(0)} + p_i t^{(1)} + p_i^2 t^{(2)} + \dots + p_i^M t^{(M)} = -c_i$ ,  $i = 1, \dots, M+1$ , defines a *cyclic hyperplane arrangement* [30] in  $\mathbb{R}^{M+1}$  with coordinates  $t^{(0)}, \dots, t^{(M)}$ .

- The hyperplane  $\mathcal{P}_{\{i_1, i_2\}}$  is given by

$$t_{\{i_1, i_2\}}^{(1)} = -(p_{i_1} + p_{i_2}) t^{(2)} - \tilde{c}_{\{i_1, i_2\}},$$

and we have

$$\theta_{i_2} - \theta_{i_1} = (p_{i_2} - p_{i_1}) (t^{(1)} - t_{\{i_1, i_2\}}^{(1)}), \quad (4)$$

so that, for  $i_1 < i_2$ ,

$$t^{(1)} \leq t_{\{i_1, i_2\}}^{(1)} \iff \theta_{i_2} \leq \theta_{i_1}.$$

Together with (2), this implies in particular that each  $\mathcal{U}_i$  is the intersection of half-spaces, and thus a closed convex set. None of these sets is empty since they all contain  $\mathcal{U}_\Omega$ . It follows in turn that each set  $\mathcal{U}_I$  (with non-empty  $I$ ) is non-empty, closed and convex (and thus in particular connected).

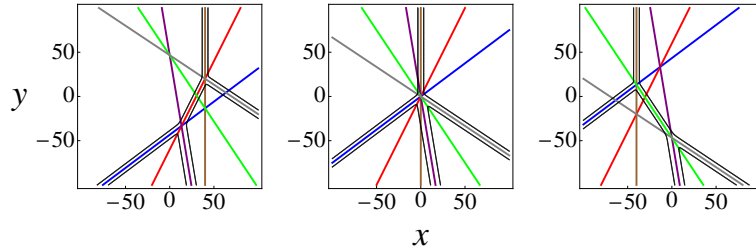


Figure 3: A soliton solution with  $M = 3$ , hence  $\Omega = \{1, 2, 3, 4\}$ , at times  $t < t_\Omega$ ,  $t = t_\Omega$  and  $t > t_\Omega$ . A thin line is the coincidence of two phases. It corresponds to some  $\mathcal{P}_{\{i, j\}}$  restricted to the respective value of  $t$ . Only a thick part of such a line is visible at the respective value of time. It corresponds to some  $\mathcal{U}_{\{i, j\}}$ , restricted to that value of  $t$ . The left and also the right plot shows two visible coincidences of three phases, corresponding to points in some  $\mathcal{U}_{\{i, j, k\}}$ . They coincide in the middle plot to form a visible four phase coincidence, the point  $\mathcal{U}_\Omega$ .

**Lemma 3.1** ([2], Proposition A.3). *For  $K = \{k_1, \dots, k_{n+1}\}$ ,  $n \in [M]$ , we have<sup>4</sup>*

$$t_{K \setminus \{k_j\}}^{(n-1)} - t_{K \setminus \{k_l\}}^{(n-1)} = (p_{k_j} - p_{k_l})(t^{(n)} - t_K^{(n)}) \quad j, l \in \{1, \dots, n+1\}.$$

With the help of this important lemma, we obtain the following result.

**Proposition 3.2.** *If  $K = \{k_1, \dots, k_{n+1}\}$  is in linear order, i.e.  $k_1 < k_2 < \dots < k_{n+1}$ , then*

$$\begin{aligned} t_{K \setminus \{k_{n+1}\}}^{(n-1)} < t_{K \setminus \{k_n\}}^{(n-1)} < \dots < t_{K \setminus \{k_1\}}^{(n-1)} & \text{for } t^{(n)} < t_K^{(n)} \\ t_{K \setminus \{k_1\}}^{(n-1)} < t_{K \setminus \{k_2\}}^{(n-1)} < \dots < t_{K \setminus \{k_{n+1}\}}^{(n-1)} & \text{for } t^{(n)} > t_K^{(n)}. \end{aligned} \quad (5)$$

The first chain in (5) is in *lexicographic order*, the second in *reverse lexicographic order*, with respect to the index sets. This makes contact with *higher Bruhat orders*, see Section 4. The following result is crucial for determining (non-)visible events.

<sup>4</sup>For  $n = 1$ , this is (4), since  $t_i^{(0)} = -\theta_i$ .

**Proposition 3.3** ([2], Corollary A.6). *Let  $I = \{i_1, \dots, i_n\}$  and  $k \in \Omega \setminus I$ . On  $\mathcal{P}_I$  we have*

$$\theta_k - \theta_{i_1} = (p_k - p_{i_1}) \cdots (p_k - p_{i_n}) (t^{(n)} - t_{I \cup \{k\}}^{(n)}). \quad (6)$$

*Example 3.4.* Let  $n = 2$  and thus  $I = \{i, i'\}$  with  $i < i'$ . On  $\mathcal{P}_I$ , (6) reads

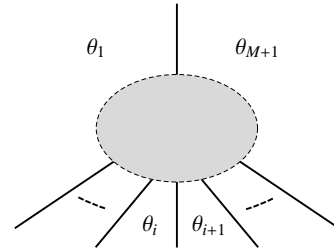
$$\theta_k - \theta_i = (p_k - p_i)(p_k - p_{i'}) (t^{(2)} - t_{\{i, i', k\}}^{(2)}).$$

If  $I$  is an interval, i.e.  $i' = i + 1$ , we have either  $k < i$  or  $k > i + 1$ , and thus  $\theta_k \leq \theta_i$  iff  $t^{(2)} \leq t_{\{i, i+1, k\}}^{(2)}$ . As a consequence, the part of  $\mathcal{P}_{\{i, i+1\}}$  with  $t^{(2)} \leq \min_k \{t_{\{i, i+1, k\}}^{(2)}\}$  is visible and the part with  $t^{(2)} > \min_k \{t_{\{i, i+1, k\}}^{(2)}\}$  is non-visible. If  $I$  is not an interval, then there is a  $k \in \{2, \dots, M\}$  such that  $i < k < i'$ . It follows that  $\theta_k > \theta_i$  if  $t^{(2)} < t_{\{i, i', k\}}^{(2)}$ , so the part of  $\mathcal{P}_{\{i, i'\}}$  with  $t^{(2)} < \max_k \{t_{\{i, i', k\}}^{(2)} \mid i < k < i'\}$  is non-visible. If there is a  $k \in \{1, \dots, M+1\}$  with  $k < i$  or  $k > i'$ , then the situation is as in the case of an interval. In the remaining case  $I = \{1\} \cup \{M+1\}$ , the part of  $\mathcal{P}_{\{1, M+1\}}$  with  $t^{(2)} \geq \max_k \{t_{\{i, i', k\}}^{(2)}\}$  is visible. We conclude that  $\mathcal{P}_I$ , with  $I$  of the form  $\{i, i+1\}$ ,  $i \in \{1, \dots, M\}$ , has a visible part extending to arbitrary negative values of  $y = t^{(2)}$ , and only  $\mathcal{P}_{\{1, M+1\}}$  has a visible part extending to arbitrary positive values of  $y$ . Any visible part of another  $\mathcal{P}_{\{i, i'\}}$  has to be bounded in the  $xy$ -plane. Furthermore, (5) shows that

$$t_{\{1,2\}}^{(1)} < t_{\{2,3\}}^{(1)} < \cdots < t_{\{M, M+1\}}^{(1)} \quad \text{for} \quad t^{(2)} < \min_{i,k} \{t_{\{i, i+1, k\}}^{(2)}\}.$$

All this information determines the asymptotic line soliton structure in the  $xy$ -plane depicted in Figure 4.

Figure 4: Asymptotic structure in the  $xy$ -plane ( $x = t^{(1)}$  horizontal,  $y = t^{(2)}$  vertical coordinate) for the line soliton solutions given by (1). Outside a large enough disk, the  $xy$ -plane is divided into regions as shown in the figure, where one of the phases  $\theta_i$  dominates all others. This structure is independent of the values of  $t^{(r)}$ ,  $r > 2$ .



For  $k \leq l$ , let  $[k, l]$  denote the *interval*  $\{k, k+1, \dots, l\}$ . We call an interval *even* (respectively *odd*) if its cardinality is even (respectively odd). Now we formulate a generalization of results in Example 3.4. The proof is by inspection of (6), which depends on the structure of  $I$ . We note that an even interval cannot influence the sign of the right hand side of (6).

**Proposition 3.5.** *Let  $I$  be an  $n$ -subset of  $\Omega = [M+1]$ ,  $1 < n < M+1$ .*

(1) *Let  $I$  be the disjoint union of even intervals, and also  $\{1\}$  if  $n$  is odd. Then*

$$\{t \in \mathcal{P}_I \mid t^{(n)} \leq \min\{t_K^{(n)} \mid K \in \binom{\Omega}{n+1}, I \subset K\}\}$$

*is visible, but its complement*

$$\{t \in \mathcal{P}_I \mid t^{(n)} > \min\{t_K^{(n)} \mid K \in \binom{\Omega}{n+1}, I \subset K\}\}$$

*not.*

(2) *Let  $I$  be the disjoint union of  $\{M+1\}$  and any number of even intervals, and also  $\{1\}$  if  $n$  is even. Then*

$$\{t \in \mathcal{P}_I \mid t^{(n)} \geq \max\{t_K^{(n)} \mid K \in \binom{\Omega}{n+1}, I \subset K\}\}$$

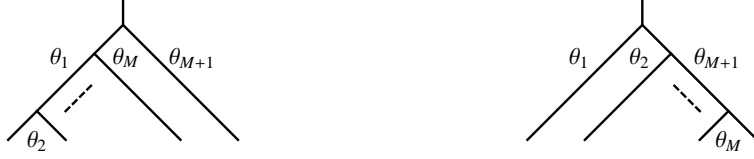


Figure 5: For sufficiently large negative (respectively positive) values of time  $t = t^{(3)}$ , any line soliton solution from the class (1) has the tree shape in the  $xy$ -plane shown by the left (right) graph.

is visible, but its complement

$$\{\mathbf{t} \in \mathcal{P}_I \mid t^{(n)} < \max\{t_K^{(n)} \mid K \in \binom{\Omega}{n+1}\}, I \subset K\}$$

not.

(3) If  $I$  is not of the form specified in (1) or (2), a visible part of  $\mathcal{P}_I$  can only appear for  $t^{(n)}$  between  $\min\{t_K^{(n)} \mid K \in \binom{\Omega}{n+1}\}, I \subset K\}$  and  $\max\{t_K^{(n)} \mid K \in \binom{\Omega}{n+1}\}, I \subset K\}$ .

*Example 3.6.* Let  $n = 3$ . According to Proposition 3.5, for  $t^{(3)} \leq \min\{t_K^{(3)} \mid K \in \binom{\Omega}{4}\}$  only (the corresponding parts of)  $\mathcal{P}_{\{1,i,i+1\}}$ ,  $i = 2, \dots, M$ , are visible, and for  $t^{(3)} \geq \max\{t_K^{(3)} \mid K \in \binom{\Omega}{4}\}$  only (the corresponding parts of)  $\mathcal{P}_{\{i,i+1,M+1\}}$ ,  $i = 1, \dots, M-1$ , are visible. The order of the values  $t_{\{1,i,i+1\}}^{(2)}$ , respectively  $t_{\{i,i+1,M+1\}}^{(2)}$ , follows from (5). All this leads to the structure of a line soliton solution for large negative time (left comb), respectively large positive time (right comb), shown in Figure 5.

*Example 3.7.* Let  $M = 5$  and  $n = 4$ . For  $t^{(4)} \leq \min\{t_K^{(4)} \mid K \in \binom{[6]}{5}\}$ , the corresponding part of  $\mathcal{P}_I$  is only visible if  $I$  is one of the sets  $\{1, 2, 3, 4\}$ ,  $\{1, 2, 4, 5\}$ ,  $\{1, 2, 5, 6\}$ ,  $\{2, 3, 4, 5\}$ ,  $\{2, 3, 5, 6\}$ ,  $\{3, 4, 5, 6\}$ . For  $t^{(4)} \geq \max\{t_K^{(4)} \mid K \in \binom{[6]}{5}\}$ , the corresponding part of  $\mathcal{P}_I$  is only visible if  $I$  is one of  $\{1, 2, 3, 6\}$ ,  $\{1, 3, 4, 6\}$ ,  $\{1, 4, 5, 6\}$ . Also see Figure 16.

In the following,  $K$  denotes the set  $\{k_1, \dots, k_{n+1}\}$ , and will be assumed to be in linear order, so that  $k_1 < \dots < k_{n+1}$ . We split such a set into<sup>5</sup>

$$\begin{aligned} K_{<} &= \{k_{n-2r} \mid r = 0, \dots, \lceil n/2 \rceil - 1\} = \{k_{2-(n \bmod 2)}, \dots, k_n\}, \\ K_{>} &= \{k_{n-2r+1} \mid r = 0, \dots, \lfloor n/2 \rfloor\} = \{k_{1+(n \bmod 2)}, \dots, k_{n+1}\}. \end{aligned}$$

Choosing a point  $\mathbf{t}_0 \in \mathcal{P}_K$  means fixing the free coordinates on  $\mathcal{P}_K$  to values  $t_0^{(n+1)}, \dots, t_0^{(M)}$ . For each  $k \in K$ , it determines a line

$$\{\mathbf{t}_{K \setminus \{k\}}(\lambda, t_0^{(n+1)}, \dots, t_0^{(M)}) \mid \lambda \in \mathbb{R}\} \subset \mathcal{P}_{K \setminus \{k\}}.$$

**Proposition 3.8** ([2], Proposition A.7). *The following half-lines are non-visible:*

$$\begin{aligned} &\{\mathbf{t}_{K \setminus \{k\}}(\lambda, t_0^{(n+1)}, \dots, t_0^{(M)}) \mid \lambda < t_K^{(n)}(t_0^{(n+1)}, \dots, t_0^{(M)})\} \text{ for } k \in K_{<}, \\ &\{\mathbf{t}_{K \setminus \{k\}}(\lambda, t_0^{(n+1)}, \dots, t_0^{(M)}) \mid \lambda > t_K^{(n)}(t_0^{(n+1)}, \dots, t_0^{(M)})\} \text{ for } k \in K_{>}. \end{aligned}$$

**Proposition 3.9.** *If  $\mathbf{t}_0 = \mathbf{t}_I(t_0^{(n)}, \dots, t_0^{(M)})$  is non-visible, then there is a  $k \in \Omega \setminus I$  such that  $\mathbf{t}_0$  lies on the non-visible side of the point  $\mathbf{t}_{I \cup \{k\}}(t_0^{(n+1)}, \dots, t_0^{(M)})$  on the line  $\{\mathbf{t}_I(\lambda, t_0^{(n+1)}, \dots, t_0^{(M)}) \mid \lambda \in \mathbb{R}\}$ .*

<sup>5</sup> $\lceil n/2 \rceil$  denotes the smallest integer greater than or equal to  $n/2$ , and  $\lfloor n/2 \rfloor$  the largest integer smaller than or equal to  $n/2$ .



*Proof.* Since  $\mathbf{t}_0$  is non-visible, it lies in some  $\mathcal{U}_k$ ,  $k \notin I$ . Let  $K = I \cup \{k\}$ . Then  $\mathbf{t}_1 := \mathbf{t}_K(t_0^{(n+1)}, \dots, t_0^{(M)})$  lies on the above line. Let us consider the case  $t_0^{(n)} < t_K^{(n)}(t_0^{(n+1)}, \dots, t_0^{(M)})$ . If  $k \in K_>$ , then (6) shows that  $\theta_k < \theta_{i_1}$ , which contradicts  $\mathbf{t}_0 \in \mathcal{U}_k$ . Hence  $k \in K_<$  and  $\mathbf{t}_0$  lies on the non-visible side of  $\mathbf{t}_1$  according to Proposition 3.8. A similar argument applies in the case  $t_0^{(n)} > t_K^{(n)}(t_0^{(n+1)}, \dots, t_0^{(M)})$ .  $\square$

According to Proposition 3.9, Proposition 3.8 provides us with a method to determine *all* non-visible points, and thus also all visible points.

A point  $\mathbf{t}_0 \in \mathcal{P}_I$  is called *generic* if  $\mathbf{t}_0 \notin \mathcal{P}_J$  for every  $J \subset \Omega$ ,  $J \not\subset I$ .

**Proposition 3.10.** *Let  $\mathbf{t}_0 \in \mathcal{P}_I$  be generic and visible, and  $U$  any convex neighborhood of  $\mathbf{t}_0$  in  $\mathcal{P}_I$  that does not intersect any  $\mathcal{P}_K$  with  $I \subset K$ ,  $I \neq K$ . Then  $U$  is visible.*

*Proof.* Let  $U$  be a neighborhood as specified in the assumptions. Suppose a non-visible point  $\mathbf{t}_1 \in U$  exists. Then there is some  $k \in \Omega \setminus I$  such that, at  $\mathbf{t}_1$ ,  $\theta_k$  dominates all phases associated with elements of  $I$ . Let  $\mathbf{t}'$  be the point where the line segment connecting  $\mathbf{t}_0$  and  $\mathbf{t}_1$  intersects the boundary of  $\mathcal{U}_k$ . Then  $\mathbf{t}' \in U \cap \mathcal{U}_k \subset \mathcal{P}_{I \cup \{k\}}$  contradicts one of our assumptions.  $\square$

**Proposition 3.11.** *If  $\mathbf{t}_0 \in \mathcal{P}_K$  is generic and visible, then points sufficiently close to  $\mathbf{t}_0$  on the complementary half-line of any of the half-lines in Proposition 3.8 are also visible.*

*Proof.* We have  $\mathbf{t}_0 \in \mathcal{U}_{k_r}$ ,  $r = 1, \dots, n+1$ . The lines

$$\mathcal{L}_r = \{\mathbf{t}_{K \setminus \{k_r\}}(\lambda, t_0^{(n+1)}, \dots, t_0^{(M)}) \mid \lambda \in \mathbb{R}\} \quad r = 1, \dots, n+1$$

all lie in the  $n$ -dimensional space  $\mathcal{E}$  defined by  $t^{(s)} = t_0^{(s)}$ ,  $s = n+1, \dots, M$ . Since  $\mathbf{t}_0$  is assumed to be visible and generic, there is a neighborhood of  $\mathbf{t}_0$  covered by the sets  $\mathcal{U}_{k_r} \cap \mathcal{E}$ . Since each line contains the visible point  $\mathbf{t}_0$ , its visible part extends on the complementary side of that in Proposition 3.8, either indefinitely or until it meets some  $\mathcal{U}_m$  with  $m \notin K$ .  $\square$

**Proposition 3.12.** *Let  $I \in \binom{\Omega}{n}$ ,  $n \in \{1, \dots, M\}$ , and  $t_0^{(n+1)}, \dots, t_0^{(M)} \in \mathbb{R}$ .*

*If all points  $\mathbf{t}_{I \cup \{k\}}(t_0^{(n+1)}, \dots, t_0^{(M)})$ ,  $k \in \Omega \setminus I$ , are non-visible, then the whole line*

$$\{\mathbf{t}_I(\lambda, t_0^{(n+1)}, \dots, t_0^{(M)}) \mid \lambda \in \mathbb{R}\}$$

*is non-visible.*

*Proof.* Suppose there is a visible point  $\mathbf{t}_0 = \mathbf{t}_I(\lambda_0, t_0^{(n+1)}, \dots, t_0^{(M)})$  on the above line, which we denote as  $\mathcal{L}$ . Let  $\mathbf{t}_1 := \mathbf{t}_{I \cup \{m\}}(t_0^{(n+1)}, \dots, t_0^{(M)})$  be the nearest of the non-visible points specified in the assumption. Then there is some  $m' \in \Omega \setminus I$ ,  $m' \neq m$ , such that  $\mathbf{t}_1 \in \mathcal{U}_{m'} \cap \mathcal{L}$ . The line segment between  $\mathbf{t}_0$  and  $\mathbf{t}_1$  meets the boundary of the convex set  $\mathcal{U}_{m'}$  at the point  $\mathbf{t}_{I \cup \{m'\}}(t_0^{(n+1)}, \dots, t_0^{(M)})$ . Since the latter would then be visible, we have a contradiction.  $\square$

**Proposition 3.13.** *For each  $I \in \binom{\Omega}{n}$ ,  $n \in \{1, \dots, M\}$ , there are  $t_0^{(n+1)}, \dots, t_0^{(M)} \in \mathbb{R}$  such that the line  $\{\mathbf{t}_I(\lambda, t_0^{(n+1)}, \dots, t_0^{(M)}) \mid \lambda \in \mathbb{R}\}$  has a visible part.*

*Proof.* Since  $\mathcal{P}_\Omega$  is a visible point, we can use Proposition 3.11 iteratively.  $\square$

Now we arrived at the following situation. From Proposition 3.2, we recall that

$$\begin{aligned} t_{K \setminus \{k_{n+1}\}}^{(n-1)} &< t_{K \setminus \{k_{n-1}\}}^{(n-1)} < \cdots < t_{K \setminus \{k_{1+(n \bmod 2)}\}}^{(n-1)} && \text{for } t^{(n)} < t_K^{(n)} \\ t_{K \setminus \{k_{2-(n \bmod 2)}\}}^{(n-1)} &< \cdots < t_{K \setminus \{k_{n-2}\}}^{(n-1)} < t_{K \setminus \{k_n\}}^{(n-1)} && \text{for } t^{(n)} > t_K^{(n)}. \end{aligned} \quad (7)$$

For all  $t_{K \setminus \{k_i\}}^{(n-1)}$  that are absent in the respective chain, there is no visible event in the respective half-space ( $t^{(n)} < t_K^{(n)}$ , respectively  $t^{(n)} > t_K^{(n)}$ ). Let  $\mathbf{t}_0 \in \mathcal{P}_K$  be given by  $t^{(n)} = t_K^{(n)}$  and fixing the higher variables to  $t_0^{(n+1)}, \dots, t_0^{(M)}$ . Let  $\mathbf{t}_0$  be visible and generic, and  $t_{K \setminus \{k_i\}}^{(n-1)}$  in one of the chains in (7). For  $t^{(n)}$  close enough to  $t_K^{(n)}$ , and on the respective side according to (7), every event in  $\mathcal{P}_{K \setminus \{k_i\}}$  with remaining coordinates  $t^{(n)}, t_0^{(n+1)}, \dots, t_0^{(M)}$  is visible.

*Example 3.14.* For  $n = 3$  and  $k_1 < k_2 < k_3 < k_4$ , (7) takes the form

$$\begin{aligned} y_{\{k_1, k_2, k_3\}} &< y_{\{k_1, k_3, k_4\}} && \text{if } t \leq t_{\{k_1, k_2, k_3, k_4\}} \\ y_{\{k_2, k_3, k_4\}} &< y_{\{k_1, k_2, k_4\}} && \end{aligned}$$

Fixing all variables  $t^{(n)}$ ,  $n > 3$ , for  $t < t_{\{k_1, k_2, k_3, k_4\}}$  close enough to  $t_{\{k_1, k_2, k_3, k_4\}}$ , the corresponding points of  $\mathcal{P}_{\{k_1, k_2, k_3\}}$  and  $\mathcal{P}_{\{k_1, k_3, k_4\}}$  are visible, but not the corresponding points of  $\mathcal{P}_{\{k_2, k_3, k_4\}}$  and  $\mathcal{P}_{\{k_1, k_2, k_4\}}$ , whereas for  $t > t_{\{k_1, k_2, k_3, k_4\}}$  it is the other way around. All this describes a *tree rotation*, see the plots in Figure 2.

We described line solitons as objects moving in the  $xy$ -plane (where  $x = t^{(1)}$  and  $y = t^{(2)}$ ). They evolve according to the KP equation (with evolution parameter  $t = t^{(3)}$ ), the first equation of the KP hierarchy. A higher KP hierarchy equation has one of the parameters  $t^{(r)}$ ,  $r > 3$ , as its evolution parameter. We do not consider the corresponding evolutions in this work, but it turned out that these parameters are important in order to classify the various evolutions. We showed that solitons from a subclass have the form of rooted binary trees with leaves extending to infinity in the  $xy$ -plane and evolving by right rotation as time  $t$  proceeds. They all start with the same asymptotic form as  $t \sim -\infty$  and end with the same asymptotic form as  $t \sim +\infty$ . These are the maximal and minimal element, respectively, of a Tamari lattice, and any generic evolution thus corresponds to a maximal chain. For a soliton configuration with  $M + 1$  leaves, which chain is realized depends on the values of the parameters  $t^{(r)}$ ,  $r = 1, \dots, M$ .

## 4 Higher Bruhat and higher Tamari orders

According to Proposition 3.2, a substantial role in the combinatorics underlying the tree-shaped line solitons is played by the order relations (5). They are at the roots of the generalization by Manin and Schechtman of the weak Bruhat order on the set of permutations of  $[n]$  to ‘higher Bruhat orders’ [17–19], also see [30]. In the following subsection we recall some definitions and results mainly from [30]. In section 4.2 we introduce ‘higher Tamari orders’.

### 4.1 Higher Bruhat orders

Let  $n, N \in \mathbb{N}$  with  $1 \leq n \leq N - 1$ . An element  $K \in \binom{[N]}{n+1}$  will be written as  $K = \{k_1, \dots, k_{n+1}\}$  with  $k_1 < \cdots < k_{n+1}$ .  $P(K)$  denotes the *packet* of  $K$ , i.e. the set of  $n$ -subsets of  $K$ . The *lexicographic order* on  $P(K)$  is given by  $K \setminus \{k_{n+1}\}, K \setminus \{k_n\}, \dots, K \setminus \{k_1\}$ . A *beginning segment* of  $P(K)$  has the form  $\{K \setminus \{k_{n+1}\}, K \setminus \{k_n\}, \dots, K \setminus \{k_j\}\}$  for some  $j$ . An *ending segment* is of the form  $\{K \setminus \{k_j\}, K \setminus \{k_{j-1}\}, \dots, K \setminus \{k_1\}\}$ .<sup>6</sup>

<sup>6</sup> $\emptyset$  and  $P(K)$  are considered as being both, beginning and ending.

A subset  $U \subset \binom{[N]}{n+1}$  is called *consistent* if its intersection with any  $(n+1)$ -packet<sup>7</sup> is either a beginning or an ending segment. The *higher Bruhat order*  $B(N, n)$  is the set of consistent subsets of  $\binom{[N]}{n+1}$ , ordered by single-step inclusion.<sup>8</sup>

*Example 4.1.* The consistent subsets of  $\binom{[3]}{2}$  are  $\emptyset, \{\{1, 2\}\}, \{\{2, 3\}\}, \{\{1, 2\}, \{1, 3\}\}, \{\{1, 3\}, \{2, 3\}\}, \{\{1, 2\}, \{1, 3\}, \{2, 3\}\}$ . Single-step inclusion leads to  $B(3, 1)$ , which has a hexagonal Hasse diagram (also see Figure 7 in Section 4.2).

A linear order  $\rho$  on  $\binom{[N]}{n}$  (which may be regarded as a permutation of  $\binom{[N]}{n}$ ) is called *admissible* if, for every  $K \in \binom{[N]}{n+1}$ , the packet of  $K$  appears in it either in lexicographic or in reverse lexicographic order. Let  $A(N, n)$  be the set of admissible linear orders of  $\binom{[N]}{n}$ . Two elements  $\rho, \rho'$  of  $A(N, n)$  are *elementarily equivalent*, if they differ only by the exchange of two neighboring elements that are not contained in a common packet. The resulting equivalence relation will be denoted by  $\sim$ . For each  $\rho \in A(N, n)$ , the *inversion set*  $\text{inv}(\rho)$  is the set of all  $K \in \binom{[N]}{n+1}$  for which  $P(K)$  appears in reverse lexicographic order in  $\rho$ . We have  $\rho \sim \rho'$  iff  $\text{inv}(\rho) = \text{inv}(\rho')$ , so that the inversion set only depends on the equivalence class of  $\rho$ . All this results in a poset isomorphism  $U = \text{inv}(\rho) \mapsto [\rho]$  between  $B(N, n)$  and  $A(N, n)/\sim$ .<sup>9</sup>

For  $[\rho] \in A(N, n)/\sim$ , let  $Q[\rho]$  be the intersection of all *linear* orders in  $[\rho]$ , i.e. the partial order on  $\binom{[N]}{n}$  given by  $I' < I$  iff  $I' <_{\sigma} I$  for all  $\sigma \in [\rho]$ . The set of linear extensions of  $Q[\rho]$  coincides with  $[\rho]$ . We set  $Q(U) := Q[\rho]$  where  $U = \text{inv}(\rho)$ .

Of great help for the construction of higher Bruhat orders is the existence [17, 18, 30] of a natural bijection between  $A(N, n)$  and the set of maximal chains of  $B(N, n-1)$ , which we describe next. With  $\rho = (I_1, \dots, I_s) \in A(N, n)$  (where  $I_i \in \binom{[N]}{n}$  and  $s = \binom{[N]}{n}$ ) we associate the chain of consistent sets  $\emptyset \rightarrow \{I_1\} \rightarrow \{I_1, I_2\} \rightarrow \dots \rightarrow \{I_1, \dots, I_s\} = \binom{[N]}{n}$  in  $B(N, n-1)$ . Conversely, given a maximal chain  $\emptyset \rightarrow U_1 \rightarrow U_2 \rightarrow \dots \rightarrow \binom{[N]}{n}$  of consistent sets in  $B(N, n-1)$ , these are ordered by single step inclusion, hence  $U_{r+1} \setminus U_r = \{I_r\}$  with some  $I_r \in \binom{[N]}{n}$ . Thus we obtain an admissible linear order  $(I_1, \dots, I_s) \in A(N, n)$ . If, for some  $K \in \binom{[N]}{n+1}$ ,  $P(K)$  appears in (reverse) lexicographic order in  $\rho$ , then  $U_r \cap P(K)$  is a beginning (ending) segment, for  $r = 0, 1, \dots, s$ . Conversely, if  $U$  is an element of a maximal chain of  $B(N, n-1)$ , and if  $U \cap P(K)$  is a beginning (ending) segment, then this holds for all elements of this chain. Thus  $P(K)$  appears in the corresponding  $\rho$  in (reverse) lexicographic order. Furthermore, if two maximal chains have a common edge  $U \xrightarrow{I} U \cup \{I\}$ , then, obviously, both contain all packets having  $I$  as a member in the same way (i.e. lexicographically, respectively reverse lexicographically).

With the help of these results, all higher Bruhat orders can be constructed iteratively, starting from the highest, i.e.  $B(N, N-1)$ . The latter consists of only two elements,  $\emptyset$  and  $\{[N]\}$ .

Suppose we have constructed  $B(N, n)$ . Its elements are consistent sets of the form  $\{K_1, \dots, K_r\}$ , where  $K_i \in \binom{[N]}{n+1}$  and  $r \in \{0, 1, \dots, \binom{[N]}{n+1}\}$  ( $\emptyset$  if  $r = 0$ ). Associated with each such consistent set  $U$  is an equivalence class  $[\rho] \in A(N, n)/\sim$  such that  $U = \text{inv}(\rho)$ . For each  $\rho \in [\rho]$  we construct the corresponding maximal chain of  $B(N, n-1)$ , as explained above. The collection of all such maximal chains constitutes  $B(N, n-1)$ . Its elements are consistent sets  $\{I_1, \dots, I_r\}$ ,  $r \in \{0, 1, \dots, s\}$ . Now we can continue to construct  $B(N, n-2)$ , and so forth.

Having arrived at  $B(N, 1)$ , the weak Bruhat order on the permutation group  $S_N$ , we can even proceed once more. We consider a permutation  $\pi = (\pi_1, \pi_2, \dots, \pi_N) \in S_N$  as an order  $\{\pi_1\} < \{\pi_2\} < \dots < \{\pi_N\}$ , which in turn determines the chain  $\emptyset \rightarrow \{\{\pi_1\}\} \rightarrow \{\{\pi_1\}, \{\pi_2\}\} \rightarrow \dots \rightarrow \{\{\pi_1\}, \dots, \{\pi_N\}\} = \binom{[N]}{1}$ . These are the maximal chains of  $B(N, 0)$ , which is isomorphic to the Boolean lattice of subsets of

<sup>7</sup>An  $(n+1)$ -packet is the packet of some element of  $\binom{[N]}{n+2}$ .

<sup>8</sup>By a theorem of Ziegler [30], this definition is equivalent to the original one of Manin and Schechtman [17, 18], also see [4]. For finite sets  $U, U'$ , *single-step inclusion* is defined by  $U \subset U'$  and  $|U'| = |U| + 1$ .

<sup>9</sup>The difficult part is to show that the set of inversion sets coincides with the set of consistent sets, see [30].

$[N]$  and forms an  $N$ -cube.<sup>10</sup>

In the following, we represent a higher Bruhat order  $B(N, n)$  by a diagram, suppressing the labels of the vertices and expressing a maximal chain  $\emptyset \rightarrow \{K_1\} \rightarrow \{K_1, K_2\} \rightarrow \cdots \rightarrow \{K_1, \dots, K_q\} = \binom{[N]}{n+1}$ ,  $q = \binom{N}{n+1}$ , graphically as

$$\bullet \xrightarrow{K_1} \bullet \xrightarrow{K_2} \bullet \cdots \bullet \xrightarrow{K_q} \bullet .$$

The edges are thus labelled by the sets  $K_i$ , which are sequentially added to the preceding vertex, starting with the empty set. The vertices are thus given by sets of the form  $\{K_1, \dots, K_r\}$ ,  $r \in \{0, 1, \dots, q\}$ . They are ordered by single step inclusion, and we have  $(K_1, \dots, K_q) \in A(N, n+1)$ .

*Remark 4.2.* The weak Bruhat order  $B(N, 1)$  is a lattice and can be visualized as a polytope in  $N - 1$  Euclidean dimensions, called *permutohedron*. Not all higher Bruhat orders are lattices [30] and not all can be realized as polytopes [5].

In the context of KP line solitons, the relevance of higher Bruhat orders is evident from Proposition 3.2, as already mentioned there. For fixed  $M \in \mathbb{N}$  and parameters  $p_i, c_i$ ,  $i = 1, \dots, M + 1$ , the order  $p_1 < \cdots < p_{M+1}$  induces an order on the ‘critical values’  $t_J^{(n-1)}$ ,  $J \in \binom{\Omega}{n}$ , according to the following rule. For  $t^{(n)} < t_K^{(n)}$ , the values  $t_J^{(n-1)}$ ,  $J \in P(K)$ , are ordered lexicographically, and for  $t^{(n)} > t_K^{(n)}$  they are ordered reverse lexicographically. Via the bijection  $I \mapsto t_I^{(|I|-1)}$  of subsets of  $\Omega = [M + 1]$  and the set of critical values, this corresponds to admissible permutations on  $\binom{\Omega}{n}$ . Without further restriction of the parameters, the resulting partial order is  $B(M + 1, n)$ .

#### 4.1.1 How to obtain the poset $Q(U)$ for a consistent set $U$ : an example

This subsection explains in an elementary way the construction of the poset  $Q(U)$  for a consistent set  $U$  in the case  $N = 4$ . There is only one 3-packet, namely

$$\binom{[4]}{3} = \{\{1, 2, 3\}, \{1, 2, 4\}, \{1, 3, 4\}, \{2, 3, 4\}\},$$

and thus the following 8 consistent subsets of  $\binom{[4]}{3}$ ,

$$\begin{aligned} &\emptyset, \{\{1, 2, 3\}\}, \{\{1, 2, 3\}, \{1, 2, 4\}\}, \{\{1, 2, 3\}, \{1, 2, 4\}, \{1, 3, 4\}\}, \\ &\{\{1, 2, 3\}, \{1, 2, 4\}, \{1, 3, 4\}, \{2, 3, 4\}\}, \\ &\{\{2, 3, 4\}\}, \{\{1, 3, 4\}, \{2, 3, 4\}\}, \{\{1, 2, 4\}, \{1, 3, 4\}, \{2, 3, 4\}\}. \end{aligned}$$

Single-step inclusion results in  $B(4, 2)$ , which has an octagonal Hasse diagram (see Figure 6). The packets of the elements of  $\binom{[4]}{3}$  are given by

$$\begin{aligned} P(\{1, 2, 3\}) &= \{\{1, 2\}, \{1, 3\}, \{2, 3\}\}, & P(\{1, 2, 4\}) &= \{\{1, 2\}, \{1, 4\}, \{2, 4\}\}, \\ P(\{1, 3, 4\}) &= \{\{1, 3\}, \{1, 4\}, \{3, 4\}\}, & P(\{2, 3, 4\}) &= \{\{2, 3\}, \{2, 4\}, \{3, 4\}\}. \end{aligned}$$

For each consistent subset  $U$  of  $\binom{[4]}{3}$ , we consider a table, which displays the packet of each element of  $U$  downwards in reverse lexicographic order (and the remaining packets in lexicographic order). The left one of the following two tables describes the case  $U = \emptyset$ , hence all packets are in lexicographic order.

1 2 3	1 2 4	1 3 4	2 3 4	1 2 3	1 2 4	1 3 4	2 3 4
1 2	1 2	1 3	2 3	2 3	2 4	1 3	2 3
1 3	1 4	1 4	2 4	1 3	1 4	1 4	2 4
2 3	2 4	3 4	3 4	1 2	1 2	3 4	3 4

<sup>10</sup>More generally, the elements of  $B(N, n)$  can be represented as sets of  $n$ -faces of the  $N$ -cube [26, 27].

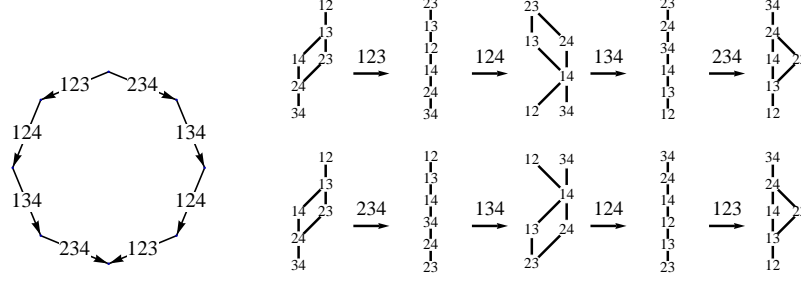


Figure 6:  $B(4, 2)$  and its two maximal chains in terms of the  $Q$ -posets, which can be constructed in the way explained in section 4.1.1.

From the table, where e.g. 12 stands for  $\{1, 2\}$ , we read off<sup>11</sup> cover relations and deduce a poset, drawn as a Hasse diagram. This leads to the very first poset (of both horizontal chains) in Figure 6. It has two linear extensions, which are elements  $\rho, \rho' \in A(4, 2)$ , one with 14, 23, the other one with 23, 14 instead. Since 14 and 23 belong to different packets,  $\rho \sim \rho'$ . Since no packet is in reverse lexicographic order,  $[\rho] \in A(4, 2)/\sim$  corresponds to the empty (consistent) set. The poset is  $Q(\emptyset)$ .

The second table above describes the case  $U = \{\{1, 2, 3\}, \{1, 2, 4\}\}$ . Its evaluation leads to  $Q(U)$ , the third poset in the first horizontal chain in Figure 6. It has four linear extensions. Since 13 and 24, as well as 12 and 34, belong to different packets, all these extensions are equivalent, hence  $U$  determines a single element of  $A(4, 2)/\sim$ . Evaluating the remaining tables, we finally obtain the two chains of posets in Figure 6.

## 4.2 Higher Tamari orders

Let  $K \in \binom{[N]}{n+1}$ . In the KP line soliton context in Section 3, where  $N = M + 1$ , we found the following rules concerning non-visible critical events. A point  $t_{K \setminus \{k\}}$  is non-visible if either (1)  $t^{(n)} < t_K^{(n)}$  and  $k \in K_<$ , or (2)  $t^{(n)} > t_K^{(n)}$  and  $k \in K_>$ . In the first case, the critical values  $t_{K \setminus \{k\}}^{(n)}$  are ordered lexicographically, in the second case reverse lexicographically. This induces a corresponding combinatorial rule on the sets that enumerate the critical values, and we can resolve the notion of ‘non-visibility’ from the special KP line soliton context as follows.

**Definition 4.3.** Let  $\rho \in A(N, n)$ .  $I \in \rho$  is called *non-visible* in  $\rho$  if there is a  $K \in \binom{[N]}{n+1}$  and a  $k \in K$  such that  $I = K \setminus \{k\}$ , and if either  $K \notin \text{inv}(\rho)$  and  $k \in K_<$ , or  $K \in \text{inv}(\rho)$  and  $k \in K_>$  (with  $K_<$  and  $K_>$  defined in Section 3).  $I$  is called *visible* in  $\rho$  if it is *not* non-visible in  $\rho$ .

Since  $\text{inv}(\rho)$  only depends on the equivalence class of  $\rho$ , this definition induces a notion of non-visibility (visibility) in  $[\rho] \in A(N, n)/\sim$ . Moreover, since an element of an admissible linear order  $\rho \in A(N, n)$  corresponds to an edge  $U \xrightarrow{I} U'$  of a maximal chain of  $B(N, n - 1)$  (cf. Section 4.1), the above definition induces a notion of non-visibility of such an edge:  $U \xrightarrow{I} U'$  is *non-visible* in a maximal chain of  $B(N, n - 1)$  if  $I = K \setminus \{k\}$  for some  $K \in \binom{[N]}{n+1}$ , and  $k \in K_<$  if  $U' \cap P(K)$  is a beginning segment,  $k \in K_>$  if  $U' \cap P(K)$  is an ending segment. If  $U \xrightarrow{I} U'$  is non-visible in one maximal chain of  $B(N, n - 1)$ , then it is non-visible in *every* maximal chain that contains it. Therefore we can drop the reference to a maximal chain.

<sup>11</sup>For example, the top node can only be an entry from the first row of the table. But the first column only leaves us with 12. It is also obvious that 34 is the bottom node. Furthermore, we see that from 13 to 24 there are two ways, via 14 respectively 23.

We have seen in Section 4.1 that any  $U \in B(N, n)$  determines a poset  $Q(U)$ . Eliminating all non-visible elements (in admissible linear orders) of  $Q(U)$ , by application of the rules in the preceding definition, results in a subposet that we denote by  $R(U)$ .

**Proposition 4.4.** *An edge  $U \xrightarrow{K} U'$  in  $B(N, n)$  is non-visible iff  $R(U) = R(U')$ .*

*Proof.* We will show that if  $U \xrightarrow{K} U'$  is non-visible, then all elements of  $P(K)$  are non-visible in (any linear extension of)  $Q(U)$  and  $Q(U')$ , and if  $U \xrightarrow{K} U'$  is visible, then  $R(U)$  and  $R(U')$  differ by elements of  $P(K)$ . Let  $I \in P(K)$ , i.e.  $K = I \cup \{k\}$  with some  $k \in [N] \setminus I$ , and  $l \in [N] \setminus K$ . We set  $L = K \cup \{l\} \in \binom{[N]}{n+2}$  and  $K' = L \setminus \{k\} \in \binom{[N]}{n+1}$ .

Let  $l \in L_{<}$ . We recall that in this case

(a)  $U' \cap P(L)$  is a beginning segment if  $U \xrightarrow{K} U'$  is non-visible,

(b)  $U' \cap P(L)$  is an ending segment if  $U \xrightarrow{K} U'$  is visible.

If  $k > l$ , then  $l \in K'_{>}$ . In case (a) we have  $K' \in U, U'$ , hence  $I = K' \setminus \{l\}$  is non-visible. In case (b) we have  $K' \notin U, U'$ , hence  $I = K' \setminus \{l\}$  is *not* non-visible with respect to  $K'$ . If  $k < l$ , then  $l \in K'_{<}$ . In case (a) we have  $K' \notin U, U'$  and  $I$  is again non-visible. In case (b) we have  $K' \in U, U'$  and  $I$  is again *not* non-visible with respect to  $K'$ .

For  $l \in L_{>}$ , we have to exchange ‘beginning’ and ‘ending’ in the above conditions (a) and (b). If  $k > l$ , we have  $l \in K'_{<}$ . Then  $I$  is non-visible in case (a) and not non-visible with respect to  $K'$  in case (b). If  $k < l$ , then  $l \in K'_{>}$ . Again,  $I$  is non-visible in case (a) and not non-visible with respect to  $K'$  in case (b).

We conclude from case (a) that non-visibility of  $U \xrightarrow{K} U'$  implies that all elements of  $P(K)$  are non-visible in  $Q(U)$ , as well as in  $Q(U')$ . Since  $K$  and all the  $K'$  exhaust the elements of  $\binom{[N]}{n+1}$  whose packets contain  $I$ , it follows from case (b) that  $I \in R(U)$  and  $I \notin R(U')$  if  $k \in K_{>}$ , whereas  $I \notin R(U)$  and  $I \in R(U')$  if  $k \in K_{<}$ .  $\square$

*Example 4.5.* Let  $N = 6, n = 3$  and  $K = 1346$ , which stands for  $\{1, 3, 4, 6\}$ . There are only two elements of  $\binom{[6]}{5}$  such that their packet contains  $K$ . These are  $L_1 = 12346$  and  $L_2 = 13456$ , hence  $l_1 = 2 \in (L_1)_{<}$  and  $l_2 = 5 \in (L_2)_{<}$ .

If  $U \xrightarrow{K} U'$  is non-visible, then  $U' \cap P(L_1)$  is a beginning segment:  $U' \cap P(L_1) = \{1234, 1236, 1246, 1346\}$ . The left table below displays the corresponding information for the construction of  $Q(U')$  and  $R(U')$ , obtained via Definition 4.3. Non-visible elements are marked in red. We see that the whole packet of  $K$  (marked in the table in light red) is already non-visible as a consequence of the information obtained from the other elements of  $\binom{[6]}{4}$ . Hence  $R(U') = R(U)$ .

If  $U \xrightarrow{K} U'$  is visible, then  $U' \cap P(L_1)$  is an ending segment:  $U' \cap P(L_1) = \{1346, 2346\}$ . In this case we obtain the right table.  $R(U)$  contains the elements 134 and 146 of  $P(K)$ . They are not present in  $R(U')$ , in which the new complementary elements 136 and 346 of  $P(K)$  show up. For  $L_2$  an analogous discussion applies. Finally we can conclude that  $R(U') \neq R(U)$ .

1234	1236	1246	1346	2346	1234	1236	1246	1346	2346
234	236	246	346	234	123	123	124	346	346
134	136	146	146	236	124	126	126	146	246
124	126	126	136	246	134	136	146	136	236
123	123	124	134	346	234	236	246	134	234

**Corollary 4.6.** *If  $U_0 \xrightarrow{K_1} U_1 \xrightarrow{K_2} \dots \xrightarrow{K_r} U_r$  is any (not necessarily maximal) chain in  $B(N, n)$ , containing at least one visible edge, then  $R(U_0) \neq R(U_r)$ .*

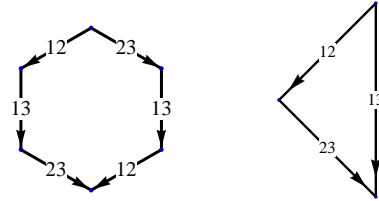
*Proof.* Without restriction of generality we can assume that  $U_0 \xrightarrow{K_1} U_1$  is visible and  $K_1 = I \cup \{k\}$  with  $k \in (K_1)_{>}$ , so that  $I \in R(U_0)$  and  $I \notin R(U_1)$ , see the proof of Proposition 4.4. Since  $K_1 \in U_s$  for  $s = 1, \dots, r$ , and  $k \in (K_1)_{>}$ ,  $I$  does not appear in any  $R(U_s)$ , and in particular not in  $R(U_r)$ .  $\square$

**Definition 4.7.** The *higher Tamari order*  $T(N, n)$  is the poset with set of vertices  $\{R(U) \mid U \in B(N, n)\}$  and the order given by  $R(U) \leq R(U')$  if  $U \leq U'$  in  $B(N, n)$ .

*Remark 4.8.* The map  $B(N, n) \rightarrow T(N, n)$ , given by  $U \mapsto R(U)$ , is surjective and order preserving. The Tamari orders also inherit the following property from the Bruhat orders. There is a bijection between the maximal chains of  $T(N, n)$  and the linear extensions of the  $R$ -posets that form the vertices of  $T(N, n + 1)$ .

In order to construct the Tamari order  $T(N, n)$ , in each of the maximal chains  $\bullet \xrightarrow{K_1} \bullet \xrightarrow{K_2} \bullet \dots \bullet \xrightarrow{K_q} \bullet$  of  $B(N, n)$  we locate the edges associated with non-visible  $K$ 's and eliminate them. This results in a reduced chain  $\bullet \xrightarrow{K_{i_1}} \bullet \xrightarrow{K_{i_2}} \bullet \dots \bullet \xrightarrow{K_{i_w}} \bullet$ .<sup>12</sup> Such an elimination involves identifying the two vertices that are connected by this edge in the Bruhat order. The consistency of this identification is guaranteed by Proposition 4.4. As a consequence of Corollary 4.6, the elimination process cannot lead to cycles, so indeed defines a partial order. Figure 7 shows a simple example.

Figure 7:  $B(3, 1)$  (weak Bruhat order on  $S_3$ ), and the corresponding Tamari order  $T(3, 1)$ . The latter is obtained from the former by eliminating in the left maximal chain the non-visible 13 and in the right maximal chain the non-visible 12 and 23.



Since  $T(N, N - 1) \cong B(N, N - 1)$ , both are represented by  $\bullet \xrightarrow{[N]} \bullet$ . For  $N = 3$  and  $N = 4$ , the vertices are represented in Figure 8, respectively Figure 9, in terms of the  $Q$ -posets, respectively  $R$ -posets, and the information contained in the latter is translated into a soliton graph.

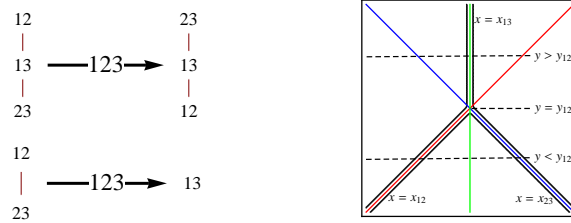


Figure 8: To the left is the poset  $B(3, 2)$  and, below it, its visible part  $T(3, 2)$ . Here the vertices are labelled by  $Q(\emptyset)$  and  $Q(\{[3]\})$ , respectively  $R(\emptyset)$  and  $R(\{[3]\})$ . The latter data translate into the soliton solution with  $M = 2$ , as indicated in the plot on the right hand side (also see [2]). At a thin line, two phases coincide. Only the thickened parts are visible. We note that  $Q(\emptyset)$  and  $Q(\{[3]\})$  are linear orders in this particular example, hence elements of  $A(3, 2)$  and, by a general result, maximal chains of  $B(3, 1)$ , see Figure 7.

<sup>12</sup>The information that resides in the edge labels of the Tamari (i.e. reduced Bruhat) chains is not sufficient to construct the  $R$ -posets, which are the vertices of  $T(N, n)$ . The latter have to be constructed from the  $Q$ -posets via elimination of non-visible elements.

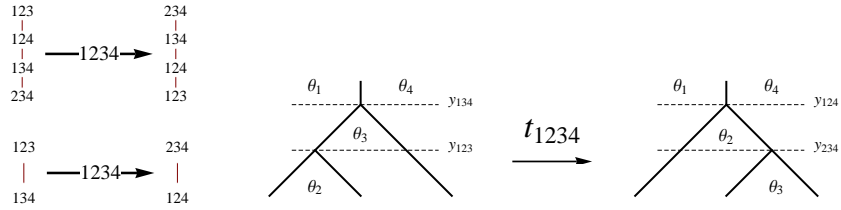


Figure 9:  $B(4, 3)$  with vertices the posets  $Q(\emptyset)$  and  $Q(\{[4]\})$ . The diagram below it is  $T(4, 3)$ , with vertices  $R(\emptyset)$  and  $R(\{[4]\})$ . To the right is the translation of  $T(4, 3)$  into a chain of two rooted binary trees related by a tree rotation. This chain is the Tamari lattice  $\mathbb{T}_2$  (in terms of rooted binary trees).

The Bruhat order  $B(N, N - 2)$  consists of two maximal chains,

$$\bullet \xrightarrow{[N-1]} \bullet \xrightarrow{[N] \setminus \{N-1\}} \bullet \dots \bullet \xrightarrow{[N] \setminus \{1\}} \bullet, \quad \bullet \xrightarrow{[N] \setminus \{1\}} \bullet \xrightarrow{[N] \setminus \{2\}} \bullet \dots \bullet \xrightarrow{[N-1]} \bullet,$$

in which  $P([N])$  appears in lexicographic, respectively reverse lexicographic order. In the first chain we have to eliminate the edges corresponding to all sets  $[N] \setminus \{k\}$  with  $k \in [N]_{<} = \{N - 1, N - 3, \dots, 1 + (N \bmod 2)\}$ , in the second chain those corresponding to such sets with  $k \in [N]_{>} = \{N, N - 2, \dots, 2 - (N \bmod 2)\}$ . This results in the two reduced chains

$$\begin{aligned} &\bullet \xrightarrow{[N-1]} \bullet \xrightarrow{[N] \setminus \{N-2\}} \bullet \dots \bullet \xrightarrow{[N] \setminus \{2 - (N \bmod 2)\}} \bullet \\ &\bullet \xrightarrow{[N] \setminus \{1 + (N \bmod 2)\}} \bullet \dots \bullet \xrightarrow{[N] \setminus \{N-3\}} \bullet \xrightarrow{[N] \setminus \{N-1\}} \bullet, \end{aligned}$$

which form  $T(N, N - 2)$ . See Figure 10 for the case  $N = 4$ . The two maximal chains of  $B(4, 2)$  with the

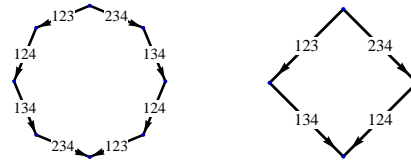


Figure 10:  $B(4, 2)$  and  $T(4, 2)$ .

$Q$ -posets as vertices have already been displayed in Figure 6. Elimination of non-visible elements yields the chains of  $T(4, 2)$  in Figure 11.

By determining the linear extensions  $K_1 \rightarrow K_2 \rightarrow \dots$  of the posets in Figure 6, we obtain maximal chains  $\bullet \xrightarrow{K_1} \bullet \xrightarrow{K_2} \dots$  of  $B(4, 1)$ . In this way we construct  $B(4, 1)$  and then obtain  $T(4, 1)$  from it by elimination of non-visible edges, see Figure 12. Figure 13 shows the corresponding construction of  $T(5, 2)$  from  $B(5, 2)$ .

#### 4.2.1 An $(n + 1)$ -gonal equivalence relation

The vertices of  $B(N, n)$  can be described by the  $Q$ -posets, and on this level we defined the transition to  $T(N, n)$ . But the vertices of  $B(N, n)$  are equivalently given by consistent sets (which was in fact our original definition). Along a maximal chain, moving from a vertex to the next means increasing the consistent set associated with the first vertex by inclusion of a new set which we use to label the edge between the two vertices. The transition from a Bruhat to a Tamari order means elimination of some of these sets. Whereas



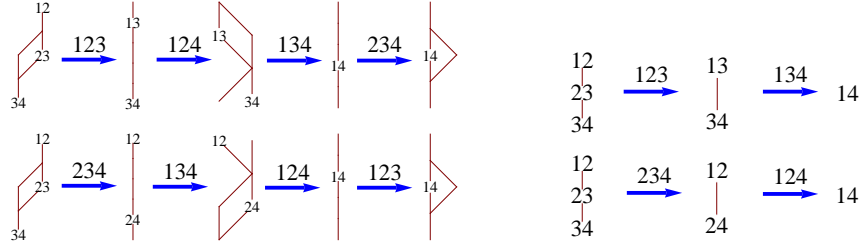


Figure 11: The two maximal chains of  $T(4, 2)$  are displayed on the right hand side. On the left hand side, in order to illustrate Proposition 4.4, we show an intermediate elimination step applied to the  $B(4, 2)$ -chains of  $Q$ -posets in Figure 6. Here we still kept the edges 124 and 234 in the upper chain, and 134, 123 in the lower chain, which are non-visible in the Tamari order. We observe that they indeed connect identical posets.

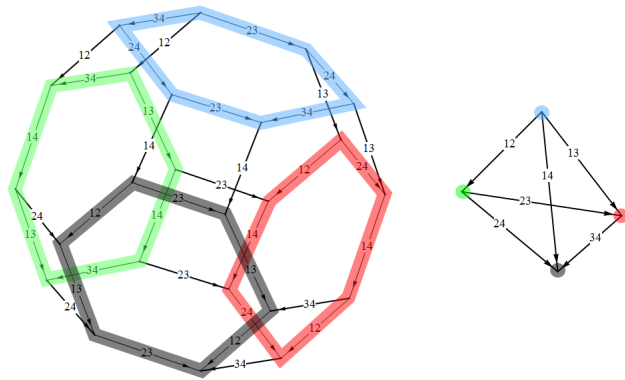


Figure 12: The left figure shows  $B(4, 1)$ . Non-visible edges connecting vertices that are mapped to the same vertex of  $T(4, 1)$  (tetrahedral poset) are marked with the same color.

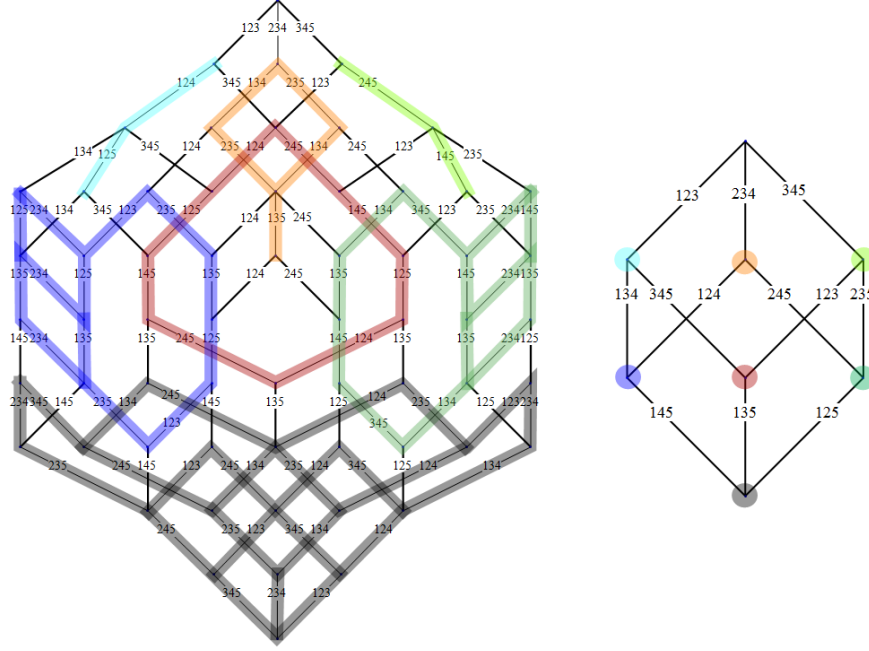
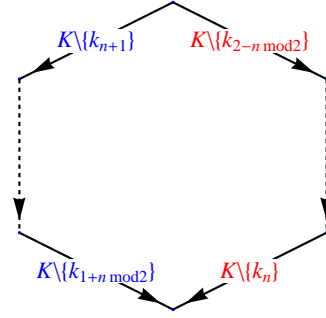


Figure 13:  $B(5, 2)$  and  $T(5, 2)$ . Vertices of  $B(5, 2)$  connected by edges marked with the same color are mapped to the same vertex of  $T(5, 2)$ .

every maximal chain of  $B(N, n)$  ends in the same set, this is not so for different Tamari chains because of different eliminations along different chains, see Figure 14. If  $U$  is the set that corresponds to the first vertex

Figure 14: For  $K \in \binom{[N]}{n+1}$ , the two chains of the diagram start in the same vertex and end in the same vertex, which includes the union of all sets associated with the edges of the left chain, but also the union of all sets associated with the edges of the right chain. The two resulting sets have to be identified, which leads to an  $(n + 1)$ -gonal equivalence relation. If  $K = \{[N]\}$ , i.e.  $n = N - 1$ , the chains are the two maximal chains of  $T(N, N - 2)$ .



from which the two chains in Figure 14 descend, the first ends in  $U \cup (K \setminus \{k_{n+1}\}) \cup \dots \cup (K \setminus \{k_{1+n \bmod 2}\})$ , the second in  $U \cup (K \setminus \{k_{2-n \bmod 2}\}) \cup \dots \cup (K \setminus \{k_n\})$ . The two resulting sets have to be identified, since the final vertex is the same. This requires the  $(n + 1)$ -gonal equivalence relation

$$U \cup \{K \setminus \{k_{n+1}\}, \dots, K \setminus \{k_{1+n \bmod 2}\}\} \sim U \cup \{K \setminus \{k_n\}, \dots, K \setminus \{k_{2-n \bmod 2}\}\},$$

for a Tamari order, and motivates the algebraic structure considered in Section 7.

## 5 KP line soliton evolutions in the case $M = 5$

For  $M = 5$  (i.e.,  $N = 6$ ) the  $\tau$ -function of a tree-shaped line soliton solution is given by

$$\tau = e^{\theta_1} + \dots + e^{\theta_6}, \quad \theta_i = p_i x + p_i^2 y + p_i^3 t + p_i^4 t^{(4)} + p_i^5 t^{(5)} + c_i,$$

with real constants  $p_1 < \dots < p_6$  and  $c_i$ . We have  $\Omega = [6] = \{1, 2, 3, 4, 5, 6\}$ , and  $\bullet \xrightarrow{[6]} \bullet$  represents  $B(6, 5)$  and also  $T(6, 5)$ . The evolution of the soliton corresponds to the left vertex if  $t^{(5)} < t_{123456}^{(5)}$ , and to the right vertex if  $t^{(5)} > t_{123456}^{(5)}$ . Associated with the two vertices are maximal chains of  $B(6, 4)$ , from which  $T(6, 4)$  is obtained by elimination of non-visible events, see Figure 15. If  $t^{(5)} < t_{123456}^{(5)}$ , the left

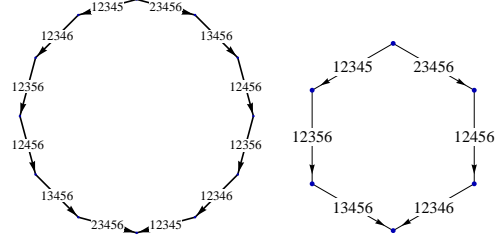


Figure 15:  $B(6, 4)$  and  $T(6, 4)$ . Here e.g. 12356 (which stands for  $\{1, 2, 3, 5, 6\}$ ) translates to the value  $t_{12356}^{(4)}$  of the parameter  $t^{(4)}$ .

chain of  $B(6, 4)$  applies, which means

$$t_{12345}^{(4)} < t_{12346}^{(4)} < t_{12356}^{(4)} < t_{12456}^{(4)} < t_{13456}^{(4)} < t_{23456}^{(4)},$$

where the second, fourth and sixth value corresponds to a non-visible event. If  $t^{(5)} > t_{123456}^{(5)}$ , the right chain of  $B(6, 4)$  applies, hence

$$t_{23456}^{(4)} < t_{13456}^{(4)} < t_{12456}^{(4)} < t_{12356}^{(4)} < t_{12346}^{(4)} < t_{12345}^{(4)},$$

where the second, fourth and sixth value is non-visible. If  $t^{(5)} = t_{123456}^{(5)}$ , all the values  $t_{ijklm}^{(4)}$  coincide.

The vertices of  $T(6, 4)$  are the  $R$ -posets in Figure 16. The linear extensions of a poset determine the possible orders of critical values of time  $t = t^{(3)}$ . For example, if  $t^{(5)} > t_{123456}^{(5)}$ , the lower horizontal chain in Figure 16 applies. If furthermore  $t_{12456}^{(4)} < t^{(4)} < t_{12346}^{(4)}$  (third poset), then we have either  $t_{1234} < t_{1456} < t_{1246} < t_{2346}$  or  $t_{1456} < t_{1234} < t_{1246} < t_{2346}$  (since the poset has two linear extensions). In order to decide which of these orders is realized by the soliton, further conditions on the parameters  $p_i$  (not the  $c_i$ ) are required (see [2]). From the linear extensions of the  $R$ -posets, we obtain (the maximal chains of)  $T(6, 3)$ , which is the Tamari lattice  $\mathbb{T}_4$ . Figure 17 displays it as a (Tamari-Stasheff) polytope. In order to identify the vertices of  $T(6, 3)$ , we take the pentagonal equivalence

$$\{\{i, j, k, l\}, \{i, j, l, m\}, \{j, k, l, m\}\} \sim \{\{i, j, k, m\}, \{i, k, l, m\}\}$$

(where  $i < j < k < l < m$ ) into account (see Section 4.2.1). The binary trees labelling its vertices in Figure 1 are obtained from the  $R$ -posets, listed in Figure 18.

Figure 19 shows an example of a line soliton evolution and the caption identifies the corresponding maximal chain of  $\mathbb{T}_4$ .

In the next steps, we obtain  $T(6, 2)$  and  $T(6, 1)$ , see Figure 20. Finally,  $T(6, 0)$  is given by the Hasse diagram with two vertices, the upper connected with the lower by six edges (labelled by  $1, 2, \dots, 6$ ).

## 6 Some insights into the case $M > 5$

The subclass of tree-shaped line soliton solutions with  $M = 6$ , hence  $N = 7$  and  $\Omega = [N] = \{1, 2, 3, 4, 5, 6, 7\}$ , is given by

$$\tau = e^{\theta_1} + \dots + e^{\theta_7}, \quad \theta_i = p_i x + p_i^2 y + p_i^3 t + p_i^4 t^{(4)} + p_i^5 t^{(5)} + p_i^6 t^{(6)} + c_i.$$

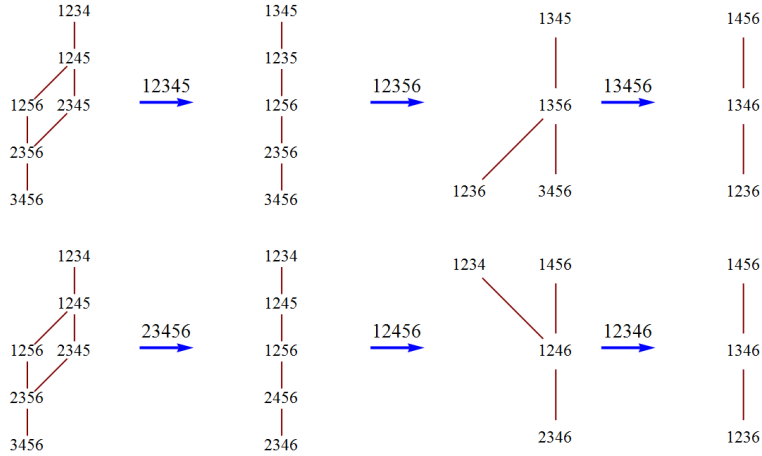


Figure 16: The two maximal chains of  $T(6, 4)$ . The vertices are the  $R$ -posets obtained from the  $Q$ -posets associated with the vertices of  $B(6, 4)$ . The upper chain applies if  $t^{(5)} < t_{123456}^{(5)}$ , the lower if  $t^{(5)} > t_{123456}^{(5)}$ .

Figure 17: The Tamari lattice  $\mathbb{T}_4 = T(6, 3)$  as a Tamari-Stasheff polytope. Such a representation first appeared in Tamari's thesis in 1951 [24].

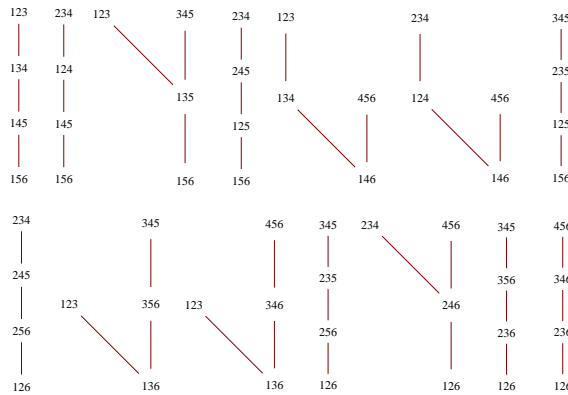
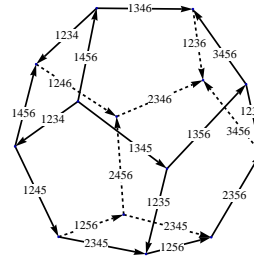


Figure 18: The fourteen  $R$ -posets that label the vertices of  $T(6, 3) = \mathbb{T}_4$ . They translate into the trees labelling the vertices of the Tamari lattice  $\mathbb{T}_4$  in Figure 1. Each poset determines more directly a triangulation of a hexagon, the vertices of which are numbered (anticlockwise) by  $1, 2, \dots, 6$ . A triple  $ijk$  then specifies a triangle.

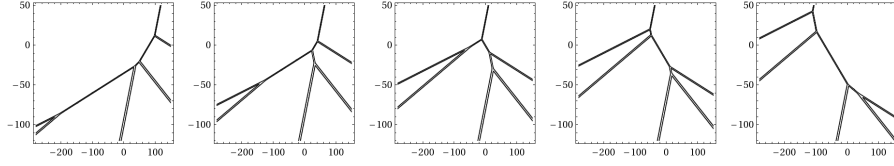


Figure 19: Plots of an  $M = 5$  soliton in the  $xy$ -plane at successive values of time. Here we have chosen the parameters such that  $t^{(5)} < t_{123456}^{(5)}$  and  $t_{12356}^{(4)} < t^{(4)} < t_{13456}^{(4)}$ . The evolution corresponds to  $\bullet \xrightarrow{1345} \bullet \xrightarrow{1356} \bullet \xrightarrow{1236} \bullet \xrightarrow{3456} \bullet$  on the Tamari lattice  $T(6, 3) = \mathbb{T}_4$  in Figure 1. It is a linear extension of the third poset of the first horizontal chain in Figure 16.

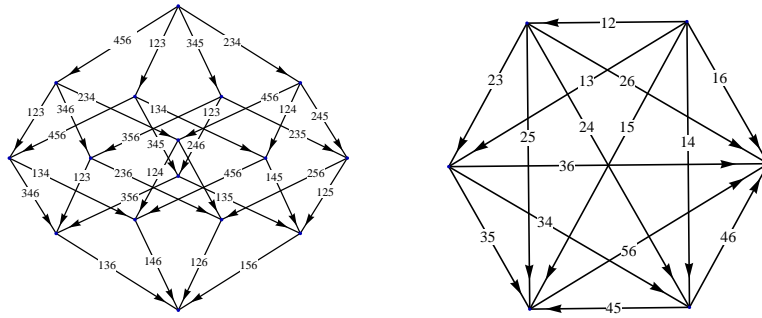


Figure 20: The Tamari order  $T(6, 2)$ , which forms a cube in four dimensions, and  $T(6, 1)$ , which is a 5-simplex.

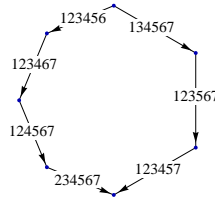


Figure 21: The Tamari order  $T(7, 5)$ .

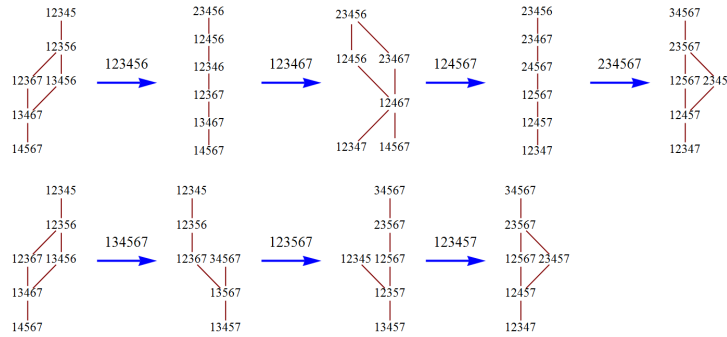


Figure 22: The two maximal chains of  $T(7, 5)$ , with vertices resolved into  $R$ -posets.

$T(7, 5)$  is the heptagon in Figure 21. The left chain is realized if  $t^{(6)} < t_{\Omega}^{(6)}$ , the right chain if  $t^{(6)} > t_{\Omega}^{(6)}$ . Each element (vertex) is an  $R$ -poset, they are displayed in Figure 22.

From these  $R$ -posets, we obtain in turn the maximal chains of  $T(7, 4)$ , hence we can construct  $T(7, 4)$  by putting all these chains together (joining a minimal and a maximal element). In this way we recover a poset that first appeared in [3] (Figure 4 therein). Using MATHEMATICA [28], we obtained a pseudo-realization as a polytope, see Figure 23.

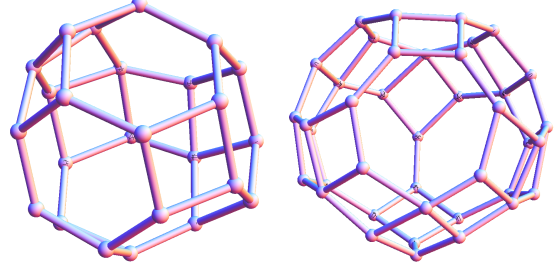


Figure 23: Polytopes on which the higher Tamari orders  $T(7, 4)$  and  $T(8, 5)$  live. It should be noticed, however, that not all faces are *regular* or *flat* quadrangles or hexagons, respectively heptagons (as also in Figure 17 with pentagons, cf. [14]).

In the next step, we obtain the Tamari lattice  $\mathbb{T}_5 = T(7, 3)$ , which can be realized as the 4-dimensional associahedron. Its maximal chains classify the possible evolutions of a tree-shaped line soliton with seven phases.

Figure 23 also shows that  $T(8, 5)$  is polytopal. Figure 24 displays polytope-like representations of some other higher Tamari orders. These are *not* polytopes, however.

## 7 An algebraic construction of higher Bruhat and Tamari orders

### 7.1 Higher Bruhat orders and simplex equations

Let  $n, N$  be integers with  $0 < n < N$ . Let  $\mathcal{B}_{N,n}$  be the monoid generated by symbols  $R_I, I \in \binom{[N]}{n}$ , and  $R_K, K \in \binom{[N]}{n+1}$ , subject to the following relations.

- (a)  $R_J R_{J'} = R_{J'} R_J$  if  $J, J' \in \binom{[N]}{k}$ ,  $k \in \{n, n+1\}$ , are such that  $|J \cup J'| > k+1$ .
- (b)  $R_I R_K = R_K R_I$  if  $I \not\subset K$ .
- (c) For  $K = \{k_1, \dots, k_{n+1}\}, k_1 < k_2 < \dots < k_{n+1}$ ,

$$R_{K \setminus \{k_{n+1}\}} R_{K \setminus \{k_n\}} \cdots R_{K \setminus \{k_1\}} = R_K R_{K \setminus \{k_1\}} R_{K \setminus \{k_2\}} \cdots R_{K \setminus \{k_{n+1}\}}. \quad (8)$$

Recall that, if two neighbors  $I_j, I_{j+1} \in \binom{[N]}{n}$  in a linear order  $\rho = (I_1, \dots, I_s) \in A(N, n)$  (where  $s = \binom{N}{n}$ ) are not contained in a common packet (or, equivalently, if  $|I_j \cup I_{j+1}| > n+1$ ), exchanging them leads to an elementarily equivalent linear order  $\rho'$ , i.e.  $\rho \sim \rho'$ . As a consequence of the above relations, the map that sends  $\rho$  to the monomial  $R_{I_1} R_{I_2} \cdots R_{I_s}$  induces a correspondence between equivalence classes  $[\rho]$ , and thus elements of the higher Bruhat order  $B(N, n)$ , and such monomials. Relation (c) encodes the order relations of  $B(N, n)$ . It relates a lexicographically ordered product to the reverse lexicographically ordered product. In the following, we write

$$R_{i_1 \dots i_n} := R_{\{i_1, \dots, i_n\}} \quad i_1 < i_2 < \dots < i_n.$$

For  $n = 1$ , we have

$$R_i R_j = R_{ij} R_j R_i \quad i < j,$$

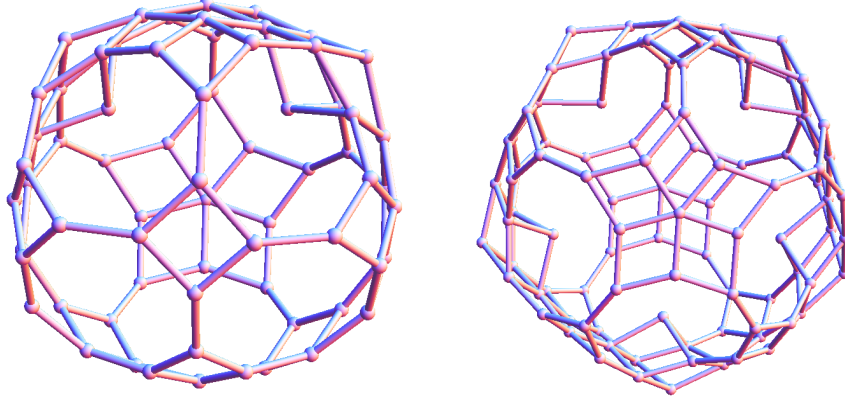


Figure 24: Polytope-like structures on which the higher Tamari orders  $T(9, 6)$  and  $T(10, 7)$  live. The existence of ‘small cubes’ (cf. [5], proof of Observation 5.3) indicates that these are *not* polytopes. There are two of them in the left figure, and five in the right.

and, for  $i < j < k$ ,

$$(R_i R_j) R_k = R_{ij} R_j (R_i R_k) = R_{ij} R_j R_{ik} R_k R_i = R_{ij} R_{ik} (R_j R_k) R_i = R_{ij} R_{ik} R_{jk} R_k R_j R_i,$$

and also

$$R_i (R_j R_k) = R_i R_{jk} R_k R_j = R_{jk} (R_i R_k) R_j = R_{jk} R_{ik} R_k (R_i R_j) = R_{jk} R_{ik} R_{ij} R_k R_j R_i.$$

Associativity now leads to the *consistency condition*

$$R_{ij} R_{ik} R_{jk} = R_{jk} R_{ik} R_{ij} \quad i < j < k. \quad (9)$$

For  $N = 3$ , this is  $R_{12} R_{13} R_{23} = R_{23} R_{13} R_{12}$ , which has the form of the *Yang-Baxter equation* [21]. (9) is a special case of (8) for  $n = 2$ ,

$$R_{ij} R_{ik} R_{jk} = R_{ijk} R_{jki} R_{ikj} \quad i < j < k.$$

This generalization of (9) has been considered in particular in [7, 10, 11, 16].

For example, in  $\mathcal{B}_{4,1}$ , we have

$$\begin{aligned} (R_1 R_2) R_3 R_4 &= R_{12} R_2 (R_1 R_3) R_4 = R_{12} R_{13} (R_2 R_3) R_1 R_4 = R_{12} R_{13} R_{23} R_3 R_2 (R_1 R_4) \\ &= R_{12} R_{13} R_{23} R_{14} R_3 (R_2 R_4) R_1 = R_{12} R_{13} R_{23} R_{14} R_{24} (R_3 R_4) R_2 R_1 \\ &= R_{12} R_{13} R_{23} R_{14} R_{24} R_{34} R_4 R_3 R_2 R_1. \end{aligned}$$

The product with which we started corresponds to the minimal element of  $B(4, 1)$ , i.e.  $(\{1\}, \{2\}, \{3\}, \{4\})$ . After a sequence of inversions, leading to new elements of  $B(4, 1)$ , the resulting product  $R_4 R_3 R_2 R_1$  corresponds to the maximal element  $(\{4\}, \{3\}, \{2\}, \{1\})$ . The final sequence of  $R_{ij}$ ’s represents an element of  $A(4, 2)$ . In  $\mathcal{B}_{4,2}$ , we have

$$\begin{aligned} (R_{12} R_{13} R_{23}) R_{14} R_{24} R_{34} &= R_{123} R_{23} R_{13} (R_{12} R_{14} R_{24}) R_{34} \\ &= R_{123} R_{124} R_{23} [R_{13} R_{24}] R_{14} [R_{12} R_{34}] = R_{123} R_{124} R_{23} R_{24} (R_{13} R_{14} R_{34}) R_{12} \\ &= R_{123} R_{124} R_{134} (R_{23} R_{24} R_{34}) R_{14} R_{13} R_{12} = R_{123} R_{124} R_{134} R_{234} R_{34} R_{24} R_{23} R_{14} R_{13} R_{12}, \end{aligned}$$

where square brackets indicate an application of a commutativity relation, and

$$R_{12}R_{13}[R_{23}R_{14}]R_{24}R_{34} = \dots = R_{234}R_{134}R_{124}R_{123} R_{34}R_{24}R_{23}R_{14}R_{13}R_{12} .$$

These calculations reproduce by stepwise inversions the two maximal chains of  $B(4, 2)$ , starting with the minimal element  $(\{1, 2\}, \{1, 3\}, \{2, 3\}, \{1, 4\}, \{3, 4\})$ , and ending with the maximal element, which is  $(\{3, 4\}, \{1, 4\}, \{2, 3\}, \{1, 3\}, \{1, 2\})$  (cf. Figure 6). As a consequence of associativity, we obtain the consistency condition

$$R_{123}R_{124}R_{134}R_{234} = R_{234}R_{134}R_{124}R_{123} .$$

The two sides of this equation represent the two elements of  $A(4, 3)$ . In  $\mathcal{B}_{4,3}$ , it generalizes to

$$R_{123}R_{124}R_{134}R_{234} = R_{1234} R_{234}R_{134}R_{124}R_{123} .$$

We expect that, more generally, the consistency conditions of (8) are given by

$$R_{L \setminus \{l_{n+2}\}} R_{L \setminus \{l_{n+1}\}} \cdots R_{L \setminus \{l_1\}} = R_{L \setminus \{l_1\}} R_{L \setminus \{l_2\}} \cdots R_{L \setminus \{l_{n+2}\}} \quad (10)$$

for  $L = \{l_1, \dots, l_{n+2}\} \in \binom{[N]}{n+2}$  in linear order. These consistency conditions have the form of generalized Yang-Baxter equations, the so-called *simplex equations* [1, 6, 12, 13, 29], see the following remark. A derivation of these equations as consistency conditions, in the way described above, apparently first appeared in [16] (called ‘obstruction method’ in [7, 20]).

*Remark 7.1.* For given positive integers  $n < N$ , we choose two finite-dimensional vector spaces  $V, W$ , and  $S_I \in V \otimes \text{End}(W)$ ,  $I \in \binom{[N]}{n}$ , with the property

$$S_I \tilde{\otimes} S_{I'} = P S_{I'} \tilde{\otimes} S_I \quad \text{if } |I \cup I'| > n + 1 ,$$

where  $P(w \tilde{\otimes} w') = w' \tilde{\otimes} w$ , and  $\tilde{\otimes}$  denotes the tensor product over  $\text{End}(W)$ . For  $K = \{k_1, \dots, k_{n+1}\} \in \binom{[N]}{n+1}$ ,  $k_1 < \dots < k_{n+1}$ , we write (8) in the form

$$S_{K \setminus \{k_{n+1}\}} \tilde{\otimes} S_{K \setminus \{k_n\}} \tilde{\otimes} \cdots \tilde{\otimes} S_{K \setminus \{k_1\}} = R S_{K \setminus \{k_1\}} \tilde{\otimes} S_{K \setminus \{k_2\}} \tilde{\otimes} \cdots \tilde{\otimes} S_{K \setminus \{k_{n+1}\}} ,$$

with some  $R \in \text{End}(\otimes^{n+1} W)$ . In components, this takes the form

$$S_{K \setminus \{k_{n+1}\}}^{a_{n+1}} S_{K \setminus \{k_n\}}^{a_n} \cdots S_{K \setminus \{k_1\}}^{a_1} = \sum_{b_1, \dots, b_{n+1}} R_{b_{n+1} \dots b_1}^{a_{n+1} \dots a_1} S_{K \setminus \{k_1\}}^{b_1} S_{K \setminus \{k_2\}}^{b_2} \cdots S_{K \setminus \{k_{n+1}\}}^{b_{n+1}} .$$

The consistency conditions are the  $(n + 1)$ -simplex equations

$$R_{L \setminus \{l_{n+2}\}} R_{L \setminus \{l_{n+1}\}} \cdots R_{L \setminus \{l_1\}} = R_{L \setminus \{l_1\}} R_{L \setminus \{l_2\}} \cdots R_{L \setminus \{l_{n+2}\}} ,$$

for all  $L = \{l_1, \dots, l_{n+2}\} \in \binom{[N]}{n+2}$ ,  $l_1 < l_2 < \dots < l_{n+2}$ . Here  $R_K \in \text{End}(\otimes^N V)$  is given by  $R$  acting non-trivially only on factors of the  $N$ -fold tensor product of  $V$  at those positions that are given by the numbers  $k_1, \dots, k_{n+1}$ .

*Remark 7.2.* Assuming an extension of the monoid  $\mathcal{B}_{N,n}$  to a unital ring of formal power series in an indeterminate  $\epsilon$ , and an expansion

$$R_K = \mathbf{1} + \epsilon \mathfrak{r}_K + \dots$$

in powers of  $\epsilon$ , from (10) we obtain to first nontrivial order (which is  $\epsilon^2$ )

$$\sum_{1 \leq a < b \leq n+2} [\mathfrak{r}_{L \setminus \{l_b\}} , \mathfrak{r}_{L \setminus \{l_a\}}] = 0 ,$$

which has the form of a *classical simplex equation* [6]. For  $N = 3$ , this is the *classical Yang-Baxter equation*

$$[\mathfrak{r}_{12}, \mathfrak{r}_{13}] + [\mathfrak{r}_{12}, \mathfrak{r}_{23}] + [\mathfrak{r}_{13}, \mathfrak{r}_{23}] = 0 .$$

The ‘classical limit’ does not work, however, on the level of the ‘obstruction equations’ (8).



## 7.2 Equations associated with higher Tamari orders

Let  $\mathcal{T}_{N,n}$  be the monoid obtained from  $\mathcal{B}_{N,n}$  by replacing (8) with the following  $(n+1)$ -gonal relations,

$$T_{K \setminus \{k_{n+1}\}} T_{K \setminus \{k_{n-1}\}} \cdots T_{K \setminus \{k_{1+(n \bmod 2)}\}} = T_K T_{K \setminus \{k_{2-(n \bmod 2)}\}} \cdots T_{K \setminus \{k_{n-2}\}} T_{K \setminus \{k_n\}}. \quad (11)$$

This means that we omit all factors in (8) with a non-visible index set.

Assuming that the corresponding statement for  $\mathcal{B}_{N,n}$  holds, it follows that these relations imply the *consistency conditions*

$$T_{L \setminus \{l_{n+2}\}} T_{L \setminus \{l_n\}} \cdots T_{L \setminus \{l_{2+(n \bmod 2)}\}} = T_{L \setminus \{l_{1+(n \bmod 2)}\}} \cdots T_{L \setminus \{l_{n-1}\}} T_{L \setminus \{l_{n+1}\}}$$

for all  $L = \{l_1, \dots, l_{n+2}\} \in \binom{[N]}{n+2}$  in linear order. These are special  $(n+2)$ -gonal relations. For  $n = 1, 2, 3, 4$ , they are listed in the following table.

$n$	$(n+1)$ -gonal relations	consistency conditions
1	$\Theta_i = X_{ij} \Theta_j$	$X_{ij} X_{jk} = X_{ik}$
2	$X_{ij} X_{jk} = Y_{ijk} X_{ik}$	$Y_{ijk} Y_{ikl} = Y_{jkl} Y_{ijl}$
3	$Y_{ijk} Y_{ikl} = T_{ijkl} Y_{jkl} Y_{ijl}$	$T_{ijkl} T_{ijlm} T_{jklm} = T_{iklm} T_{ijkm}$
4	$T_{ijkl} T_{ijlm} T_{jklm} = S_{ijklm} T_{iklm} T_{ijkm}$	$S_{ijklm} S_{ijkmq} S_{iklmq} = S_{jklmq} S_{ijlmq} S_{ijklq}$

Here we demand that the indices are ordered such that e.g.  $i < j$  for  $n = 1$  and  $i < j < k < l < m < q$  for  $n = 4$ , and we set

$$\Theta_i = T_{\{i\}}, \quad X_{ij} = T_{\{i,j\}}, \quad Y_{ijk} = T_{\{i,j,k\}}, \quad T_{ijkl} = T_{\{i,j,k,l\}}, \quad S_{ijklm} = T_{\{i,j,k,l,m\}}.$$

For example, for  $n = 3$ , the tetragonal relations imply

$$\begin{aligned} (Y_{ijk} Y_{ikl}) Y_{ilm} &= T_{ijkl} Y_{jkl} Y_{ijl} Y_{ilm} = T_{ijkl} Y_{jkl} (Y_{ijl} Y_{ilm}) = T_{ijkl} Y_{jkl} T_{ijlm} Y_{jlm} Y_{ijm} \\ &= T_{ijkl} T_{ijlm} (Y_{jkl} Y_{jlm}) Y_{ijm} = T_{ijkl} T_{ijlm} T_{jklm} Y_{klm} Y_{jkm} Y_{ijm} \\ Y_{ijk} (Y_{ikl} Y_{ilm}) &= Y_{ijk} T_{iklm} Y_{klm} Y_{ikm} = T_{iklm} Y_{ijk} Y_{klm} Y_{ikm} = T_{iklm} Y_{klm} (Y_{ijk} Y_{ikm}) \\ &= T_{iklm} Y_{klm} T_{ijkm} Y_{jkm} Y_{ijm} = T_{iklm} T_{ijkm} Y_{klm} Y_{jkm} Y_{ijm}, \end{aligned}$$

where  $i < j < k < l < m$ , and we obtain the consistency conditions for the  $T$ 's.

For  $N = 5$ , the indices of  $Y_{ijk}$  determine the three vertices of a triangle inside a pentagon, whose vertices are numbered consecutively counterclockwise from 1 to 5. A product of three  $Y$ 's of the kind that appears in the above computations corresponds to a triangulation of the pentagon, see Figure 25. The above computation starts with  $Y_{ijk} Y_{ikl} Y_{ilm}$ , i.e. the triangulation of the top vertex, and the computation proceeds step by step along the left, respectively right maximal chain.

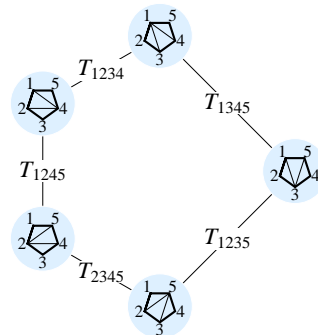


Figure 25: The two different ways of computing a product of three  $Y$ 's correspond to the maximal chains of the pentagonal lattice, which is the Tamari lattice  $\mathbb{T}_3 = T(5, 3)$ .

A particularly interesting aspect is that we can construct any of the Tamari orders  $T(N, n)$  by starting from  $X_{12}X_{23} \cdots X_{N-1,N}$ , which corresponds to the minimal element of the triangulations of the cyclic polytope  $C(N, 1)$  (see [22]). Applying the trigonal relations, we obtain from it

$$(\cdots (X_{12}X_{23}) \cdots) X_{N-2,N-1} X_{N-1,N} = Y_{123}Y_{134}Y_{145} \cdots Y_{1,N-1,N} X_{1,N} .$$

The chain of  $Y$ 's corresponds to the minimal element of the Tamari lattice  $\mathbb{T}_{N-2} = T(N, 3)$ . Elaborating all possible proper bracketings of this chain, by applications of the tetragonal relations, one obtains the maximal chains of  $T(N, 3)$ . For  $N = 6$ ,

$$(Y_{123}Y_{134})Y_{145}Y_{156} = \dots = T_{1234}T_{1245}T_{2345}T_{1256}T_{2356}T_{3456} Y_{456}Y_{346}Y_{236}Y_{126} ,$$

produces the coefficient  $T_{1234}T_{1245}T_{2345}T_{1256}T_{2356}T_{3456}$ , which we recognize as one of the longest maximal chains of the Tamari lattice  $\mathbb{T}_4$  in Figure 1. This computation moves step by step along that chain, from one tree to the next, since each product of four  $Y$ 's appearing in the computation determines the tree (which is dual to a triangulation of the 6-gon) assigned to the respective vertex. In conclusion, we have an algebraic method to construct Tamari lattices and, more generally, higher Tamari orders.

Remark 7.1 can be translated to the present setting. The significance of the equations obtained in this way has still to be explored, but an interesting observation is made in the following remark.

*Remark 7.3.* Assuming an extension of the monoid  $\mathcal{T}_{N,n}$  to a (unital) ring of formal power series in an indeterminate  $\epsilon$ , and an expansion

$$T_I = \mathbf{1} + \epsilon \mathbf{t}_I + \cdots ,$$

to first order in  $\epsilon$ , we obtain from (11) the coboundary conditions

$$\mathbf{t}_K = (\delta \mathbf{t})_K \quad \text{where} \quad (\delta \mathbf{t})_K := \mathbf{t}_{K \setminus \{k_{n+1}\}} - \mathbf{t}_{K \setminus \{k_n\}} + \mathbf{t}_{K \setminus \{k_{n-1}\}} - \cdots + (-1)^n \mathbf{t}_{K \setminus \{k_1\}} .$$

The consistency conditions are then a consequence of  $\delta^2 = 0$ . In contrast to the ‘Bruhat case’ considered in section 7.1, see Remark 7.2, in the present ‘Tamari case’ all equations possess a (formal) ‘classical limit’, which moreover turns out to be ‘cohomological’.

## 8 Further remarks

The KP equation (and its hierarchy) has connections with various areas of mathematics and (mathematical) physics. The relation with higher Bruhat and higher Tamari orders established in [2] and in the present work provides another example.

We did not explore the precise relation of the higher Tamari orders introduced in this work and the ‘higher Stasheff-Tamari posets’ of Kapranov and Voevodsky [8] (also see [3, 22]). It may well be that these orders coincide, which is indeed so for low order examples.

The higher Bruhat orders and the induced Tamari orders are supplied with a higher-dimensional category structure via the evolution variables of the KP hierarchy. It has obvious relations to Ross Street’s algebra of oriented simplexes [23] (also see [8]).

**Acknowledgement.** We would like to thank Jim Stasheff for very valuable comments and questions that led to several improvements of this work, and for his efficient proofreading.

## References

- [1] V. Bazhanov and Y. Stroganov, “Conditions of commutativity of transfer matrices on a multidimensional lattice”, *Theor. Math. Phys.* **52** (1982) 685–691.
- [2] A. Dimakis and F. Müller-Hoissen, “KP line solitons and Tamari lattices”, *J. Phys. A: Math. Theor.* **44** (2011) 025203.
- [3] P. Edelman and V. Reiner, “The higher Tamari posets”, *Mathematika* **43** (1996) 127–154.
- [4] S. Felsner and H. Weil, “A theorem on higher Bruhat orders”, *Discr. Comput. Geom.* **23** (2000) 121–127.
- [5] S. Felsner and G. Ziegler, “Zonotopes associated with higher Bruhat orders”, *Discr. Math.* **241** (2001) 301–312.
- [6] I. Frenkel and G. Moore, “Simplex equations and their solutions”, *Commun. Math. Phys.* **138** (1991) 259–271.
- [7] J. Hietarinta and F. Nijhoff, “The eight tetrahedron equations”, *J. Math. Phys.* **38** (1997) 3603–3615.
- [8] M. Kapranov and V. Voevodsky, “Combinatorial-geometric aspects of polycategory theory: pasting schemes and higher bruhat orders (list of results)”, *Cahiers de topologie et géométrie différentielle catégoriques* **32** (1991) 11–27.
- [9] Y. Kodama, “KP solitons in shallow water”, *J. Phys. A: Math. Theor.* **43** (2010) 434004.
- [10] I. Korepanov, “Tetrahedral Zamolodchikov algebras corresponding to Baxter’s  $L$ -operators”, *Comm. Math. Phys.* **154** (1993) 85–97.
- [11] ———, “The tetrahedron equation and algebraic geometry”, *J. Math. Sci.* **83** (1997) 85–92.
- [12] R. Lawrence, “Algebras and triangle relations”, *J. Pure Appl. Alg.* **100** (1995) 43–72.
- [13] ———, “Yang-Baxter type equations and posets of maximal chains”, *J. Comb. Theory, Ser. A* **79** (1997) 68–104.
- [14] J.-L. Loday, “Dichotomy of the addition of natural numbers”, *arXiv:1108.6238v1* [math.RA], to appear in the *Tamari Memorial Festschrift*.
- [15] I. Macdonald, *Symmetric functions and Hall polynomials*, 2nd ed., Oxford University Press, Oxford, 1995.
- [16] J. Maillet and F. Nijhoff, “Multidimensional lattice integrability and the simplex equations”, in *Non-linear Evolution Equations: Integrability and Spectral Methods*, A. Degasperis, A. Fordy, and M. Lakshmanan, eds., Manchester University Press, 1990, 537–548.
- [17] Y. Manin and V. Schechtman, “Arrangements of real hyperplanes and Zamolodchikov equations”, in *Group Theoretical Methods in Physics*, M. Markov, V. Man’ko, and V. Dodonov, eds., Adv. Stud. Pure Math., vol. 17, VNU Science Press, 1986, 151–165.
- [18] ———, “Higher Bruhat orders, related to the symmetric group”, *Funct. Anal. Appl.* **20** (1986) 148–150.

- [19] ———, “Arrangements of hyperplanes, higher braid groups and higher Bruhat orders”, in *Algebraic Number Theory – in honor of K. Iwasawa*, J. Coates, R. Greenberg, B. Mazur, and I. Satake, eds., Adv. Stud. Pure Math., vol. 17, Academic Press, 1989, 289–308.
- [20] F. Michielsen and F. Nijhoff, “D-algebras, the D-simplex equations, and multidimensional integrability”, in *Quantum Topology*, L. Kauffman and R. Baadhio, eds., Series on Knots and Everything, vol. 3, World Scientific, 1993, 230–243.
- [21] J. Perk and H. Au-Yang, “Yang-Baxter equations”, in *Encyclopedia of Mathematical Physics*, J.-P. Francoise, G. Naber, and S. Tsou, eds., vol. 5, Elsevier Science, 2006, 465–473.
- [22] J. Rambau and V. Reiner, “A survey of the higher Stasheff-Tamari orders”, preprint, to appear in the *Tamari Memorial Festschrift*.
- [23] R. Street, “The algebra of oriented simplexes”, *J. Pure Appl. Alg.* **49** (1987) 283–335.
- [24] D. Tamari, “Monoides préordonnés et chaînes de Malcev”, Doctorat ès-Sciences Mathématiques Thèse de Mathématique, Paris, 1951.
- [25] ———, “The algebra of bracketings and their enumeration”, *Nieuw Arch. Wisk.* **10** (1962) 131–146.
- [26] H. Thomas, “Maps between higher Bruhat orders and higher Stasheff-Tamari posets”, in *FPSAC 15th Anniversary International Conference on Formal Power Series and Algebraic Combinatorics*, K. Eriksson, A. Björner, and S. Linusson, eds., 2003.
- [27] M. Voevodski and M. Kapranov, “Free  $n$ -categories generated by a cube, oriented matroids, and higher Bruhat orders”, *Funct. Anal. Appl.* **25** (1990) 50–52.
- [28] Wolfram Research, Inc., *Mathematica 8.0*, Wolfram Research, Inc., Champaign, Illinois, 2010.
- [29] A. Zamolodchikov, “Tetrahedron equations and the relativistic  $S$ -matrix of straight-strings in 2+1-dimensions”, *Commun. Math. Phys.* **79** (1981) 489–505.
- [30] G. Ziegler, “Higher Bruhat orders and cyclic hyperplane arrangements”, *Topology* **32** (1993) 259–297.